DEUTSCHES ELEKTRONEN-SYNCHROTRON DESY

DESY 85-138
December 1985

MONTE CARLO STUDY OF THE STANDARD SU(2) HIGGS MODEL

by

W. Langguth

Institut f. Theoretische Kernphysik, Universität Karlsruhe

I. Montvay

Deutsches Elektronen-Synchrotron DESY, Hamburg

P. Weisz

II. Institut f. Theoretische Physik, Universität Hamburg

ISSN 0418-9833

NOTKESTRASSE 85 · 2 HAMBURG 52

DESY 85-138
December 1985

ISSN 0418-9833

Monte Carlo study of the standard SU(2) Higgs model

W. Langguth
Institut für Theoretische Kernphysik der Universität Karlsruhe
I. Montvay
Deutsches Elektronen-Synchrotron DESY
P. Weisz*
II. Institut für Theoretische Physik der Universität Hamburg

December 17, 1985

Abstract

The SU(2) Higgs model with scalar doublet field is numerically investigated on lattices with size between 8^4 and 12^4. Masses and zero momentum couplings are determined at several points of the three-dimensional coupling parameter space. Particular interest is given to questions related to the order of the confinement-Higgs phase transition. High statistics measurements in the region of non-perturbative scalar self-coupling and weak gauge coupling approximately equal to the physical value in the standard $SU(2) \otimes U(1)$ electro-weak theory give a Higgs-mass to W-mass ratio of 6.4 ± 0.8. The Higgs-WW coupling determined at these points is smaller than the value usually assumed in the standard model, implying that the width of the high mass Higgs-boson could still be relatively small, unless multi-W decays dominate.

1 Introduction

Our present understanding of high energy elementary particle interactions is based to a large extent on quantum gauge field theories with spin-$\frac{1}{2}$ fermion matter fields. The prototype theories are QED with the electromagnetic U(1) gauge field and the spin-$\frac{1}{2}$ electron field, and QCD with SU(3) colour gauge field and triplets of spin-$\frac{1}{2}$ quarks. Quantum field theories with scalar matter fields are usually considered to be problematic or even inconsistent. An often asked question is: can elementary scalar particles exist? The exceptional features of the weak coupling perturbation theory in supersymmetric theories may suggest, that the answer can be affirmative only in the case of supersymmetry, when there is a delicate balance between elementary fermionic and bosonic degrees of freedom.

In order to be able to answer the question about the possibility of elementary scalars, one has to consider the regularized quantum field theory. In the case of gauge fields a natural cut-off is realized by a finite space-time lattice [1], and the above question can be formulated by asking: is a lattice-regularized quantum gauge field theory with scalar matter fields mathematically consistent with a very small lattice spacing (i. e. with a cut-off much larger than the physical masses in the theory)? In the case of the simplest model with only scalar fields, namely the pure ϕ^4 model, it is almost exactly proven [2], that an infinitely high cut-off is only possible in the trivial case of free fields, without physical interaction. Models without gauge fields have, of course, only academic interest, and the inclusion of gauge fields can change the situation.

*Heisenberg foundation fellow

A simple prototype gauge model with scalar matter fields is the "standard" SU(2) Higgs model with a scalar doublet, which is an important part of the standard $SU(3) \otimes SU(2) \otimes U(1)$ theory. This and other similar Higgs models are well suited for numerical Monte Carlo studies (in fact, from the numerical point of view much simpler than gauge fields with fermions). Therefore, presently there is an increasing interest in the numerical investigation of Higgs models (for a recent review and references see [3]). The case of the standard SU(2) Higgs model is particularly simple, because the scalar doublet breaks the local gauge symmetry completely in the sense that no massless "photon" field is left over.

For zero gauge coupling the standard SU(2) Higgs model is identical to a four-component ϕ^4 model, which has presumably no non-trivial continuum limit. The inclusion of the gauge coupling could, in principle, produce a non-trivial critical point (for a non-trivial continuum limit) somewhere in the interior of the 3-dimensional coupling parameter space. (Besides the hopping parameter κ and scalar self-coupling λ of the pure ϕ^4 model the third bare coupling is $\beta \equiv 4/g^2$, which specifies the gauge field dynamics.) Recent numerical data on the correlation lengths and static energies [4,6], however, indicate that this is not probable. Moreover, the first Monte Carlo renormalization group (MCRG) study showed also no evidence for a non-trivial critical point at finite β [7]. This is not very surprising since, as a consequence of asymptotic freedom, the gauge coupling is always weak at small distances, even if it is strong at the scale of the physical masses. A non-trivial continuum limit in the standard SU(2) Higgs model can, however, exist at the critical line of the pure ϕ^4 component at $\beta = \infty$. This would be similar to the asymptotically free gauge theories with fermion matter fields, where the continuum limit is also at $\beta = \infty$.

The triviality of the pure ϕ^4 model implies that in the continuum limit the physics becomes independent of the self-coupling λ (λ is "irrelevant"). This λ-independence seems to be maintained also after the inclusion of the gauge coupling, if one considers the physical quantities, for fixed β, as a function of an appropriately chosen variable [4] (namely, the expectation value of the gauge invariant link variable). The λ-independence is an essentially non-perturbative feature which can be exactly valid only for infinitely high cut-off. For any finite cut-off there is some range of sufficiently small self-coupling, where perturbation theory in λ is expected to be applicable. In this perturbative regime there is λ-dependence. The present Monte Carlo data in the Higgs model seem to be entirely within the strongly coupled non-perturbative region, where approximate λ-independence is true.

In the present paper we report on the results of an extensive numerical Monte Carlo study of the standard SU(2) Higgs model. We shall concentrate mainly on three new aspects: some zero four-momentum coupling constants of the physical Higgs- and W-bosons, a detailed comparison of 8^4 and 12^4 data from the point of view of finite size scaling and a high statistics calculation at weak gauge coupling which roughly corresponds to the physical situation in the $SU(2) \otimes U(1)$ electro-weak theory. The scalar self-coupling is always in the non-perturbative, approximately λ-independent, region. In the next Section, after defining the notations, the obtained results for the masses and couplings on the 8^4 lattice will be summarized. Section 3 is devoted to the comparison of the behaviour near the phase transition on 8^4 and 12^4 lattices. As a part of this comparison, a finite size scaling analysis will also be carried out. In Section 4 the Monte Carlo results at weak physical gauge coupling will be presented and discussed. The last Section is reserved for a few concluding remarks.

2 Masses and couplings

2.1 Lattice action

Throughout this paper we shall use for the lattice variables the notations of Ref. [4]. In particular, the link variable for the gauge field will be denoted by $U(x,\mu) \in SU(2)$ (x = lattice point, μ = link direction), the Higgs field is specified by its length $\rho_x \geq 0$ and by an SU(2) angular variable

$\alpha_x \in SU(2)$. The lattice action in these variables can be written as

$$S_{\lambda,\beta,\kappa} = \beta \sum_P \left(1 - \frac{1}{2} Tr\, U_P\right)$$

$$+ \sum_x \left\{ \rho_x^2 - 3 \log \rho_x + \lambda(\rho_x^2 - 1)^2 - \kappa \sum_{\mu>0} \rho_{x+\hat{\mu}} \rho_x Tr\, \left(\alpha_{x+\hat{\mu}}^+ U(x,\mu) \alpha_x\right) \right\} \tag{1}$$

Here $\sum_P$ stands for a summation over positively oriented plaquettes. The integration measure corresponding to Eq. (1) is $d\rho_x\, d^3\alpha_x\, d^3U(x,\mu)$ (where d^3g denotes the Haar-measure in SU(2)). The peculiarity of the SU(2) doublet scalar field is, that its angular part is equivalent to the local gauge degree of freedom. Therefore, at any finite β it is possible to introduce, instead of the SU(2) link- and site-variables, a gauge invariant link variable

$$V(x,\mu) \equiv \alpha_{x+\hat{\mu}}^+ U(x,\mu) \alpha_x \tag{2}$$

In terms of this, the lattice action is

$$S_{\lambda,\beta,\kappa} = \beta \sum_P \left(1 - \frac{1}{2} Tr\, V_P\right) + \sum_x \left\{ \rho_x^2 - 3 \log \rho_x + \lambda(\rho_x^2 - 1)^2 - \kappa \sum_{\mu>0} \rho_{x+\hat{\mu}} \rho_x Tr\, V(x,\mu) \right\} \tag{3}$$

After performing the trivial integration over α_x, the integration measure for Eq. (3) is $d\rho_x\, d^3V(x,\mu)$.

In the limit $\lambda \to \infty$ the length of the Higgs field is frozen to unity, and the action in Eq. (1) can be replaced by

$$S_{\lambda=\infty,\beta,\kappa} = \beta \sum_P \left(1 - \frac{1}{2} Tr\, U_P\right) - \kappa \sum_{x,\mu>0} Tr\, \left(\alpha_{x+\hat{\mu}}^+ U(x,\mu) \alpha_x\right) \tag{4}$$

whereas, instead of Eq. (3) one can use

$$S_{\lambda=\infty,\beta,\kappa} = \beta \sum_P \left(1 - \frac{1}{2} Tr\, V_P\right) - \kappa \sum_{x,\mu>0} Tr\, V(x,\mu) \tag{5}$$

2.2 Monte Carlo measurement of the masses and couplings

The masses are extracted in the Monte Carlo calculation from the exponential decay of two-point correlation functions. In the Higgs-boson (scalar, isoscalar) channel we used the diagonal correlations of the quantities

$$h_x = \begin{cases} h_x^{(1)} \equiv \rho_x & \\ h_x^{(2)} \equiv Tr\, V(x,\mu) & (\mu = 1,2,3,4) \\ h_x^{(3)} \equiv \rho_{x+\hat{\mu}} \rho_x Tr\, V(x,\mu) & (\mu = 1,2,3,4) \end{cases} \tag{6}$$

In the W-boson (vector, isovector) channel correlations of

$$w_{xr\mu} = \begin{cases} w_{xr\mu}^{(1)} \equiv Tr\, (\tau_r V(x,\mu)) \\ w_{xr\mu}^{(2)} \equiv \rho_{x+\hat{\mu}} \rho_x Tr\, (\tau_r V(x,\mu)) \end{cases} \tag{7}$$

were considered (τ_r denotes a Pauli-matrix). The Monte Carlo calculations show that the three Higgs-boson, respectively, two W-boson channels are strongly correlated, that is, the masses determined in the same channel by different quantities deviate from each other much less than the individual statistical errors.

The zero momentum couplings are usually defined on the lattice in such a way that no multiplicative wave-function renormalization is left over. In the case of the n-Higgs-boson coupling Λ_{nH} the definition is (for $n \geq 3$):

$$a^{4-2n}\Lambda_{nH} \equiv \frac{\frac{1}{N}\sum_{x_1\ldots x_n}\langle h_{x_1}\ldots h_{x_n}\rangle^c}{\left[\frac{1}{N}\sum_{x_1x_2}\langle h_{x_1}h_{x_2}\rangle^c\right]^{n/2}} \tag{8}$$

Here a is the lattice spacing, N the number of lattice sites, $\langle\cdots\rangle^c$ means connected part of the expectation value, and h_x is one of the interpolating fields for the Higgs-boson in Eq. (6). Multiplying Eq. (8) by the appropriate power $(am_H)^{2n-4}$ of the Higgs-boson mass, one obtains the dimensionless quantity

$$l_{nH} \equiv m_H^{2n-4}\Lambda_{nH} \tag{9}$$

Since the coupling Λ_{nH} is defined off-mass-shell (at $p=0$), its value is not independent of the choice of the interpolating field h_x. Only the corresponding on mass shell coupling is independent, and has an immediate physical meaning. The best estimate of the physical couplings of some particular state can be obtained by using the correlations of those quantities, which are most dominated by that state.

Let us note that the zero momentum coupling λ_{nH} usually considered in weak coupling perturbation theory is not exactly the same as Λ_{nH}, because it is "truncated" by n propagators (and not by $n/2$). One can, however, consider ratios of Λ_{nH}, which coincide with the corresponding ratios of λ_{nH}, for instance,

$$\rho_{(3)nH} \equiv \frac{\Lambda_{nH}}{|\Lambda_{3H}|^{n/3}} = \frac{\lambda_{nH}}{|\lambda_{3H}|^{n/3}} \tag{10}$$

The Higgs-WW coupling is decisive for the decay of the Higgs-boson, if it is heavier than twice the W-boson. On the lattice, in analogy to Eq. (8), the zero four-momentum Higgs-WW coupling can be defined as

$$a^{-2}\Lambda_{HWW} \equiv \frac{\frac{1}{N}\sum_{x_1x_2x_3}\sum_{r\mu}\langle h_{x_1}w_{x_2r\mu}w_{x_3r\mu}\rangle^c}{\left[\frac{1}{N}\sum_{x_1x_2}\langle h_{x_1}h_{x_2}\rangle^c\right]^{1/2}\frac{1}{N}\sum_{x_2x_3}\sum_{r\mu}\langle w_{x_2r\mu}w_{x_3r\mu}\rangle^c} \tag{11}$$

Here $w_{xr\mu}$ is one of the interpolating fields for the W-boson in Eq. (7). A dimensionless quantity corresponding to Λ_{HWW} is, for instance,

$$l_{HWW} \equiv m_H m_W \Lambda_{HWW} \tag{12}$$

The numerical problem in the calculation of the zero momentum couplings in Eqs. (8,11) is the strong cancellation involved by taking the connected part. In order to see this more explicitly, let us consider, for instance, Eq. (8) in more detail. Let us denote the lattice average of the interpolating field h_x by $\bar{h}$:

$$\bar{h} = \frac{1}{N}\sum_x h_x \tag{13}$$

Note that $\bar{h}$ is proportional to the zero momentum component of h_x. In terms of $\bar{h}$ the connected part in Eq. (8) is:

$$\frac{1}{N}\sum_{x_1\ldots x_n}\langle h_{x_1}\ldots h_{x_n}\rangle^c = N^{n-1}\langle\bar{h}^n\rangle^c \tag{14}$$

Therefore we have ($n \geq 3$):

$$a^{4-2n}\Lambda_{nH} = N^{\frac{n}{2}-1}\frac{\langle\bar{h}^n\rangle^c}{\{\langle\bar{h}^2\rangle^c\}^{\frac{n}{2}}} \tag{15}$$

The cancellation involved in Eqs. (14) and (15) is displayed by the large factors given by the powers of the number of lattice points (N).

In order to obtain $\langle\bar{h}^n\rangle^c$, one can proceed (at least) in two different practical ways. The first is to calculate $\langle\bar{h}^n\rangle$ in a straightforward way for different binnings of the sweeps and determine the connected part $\langle \bar{h}^n\rangle^c$ from the sweeps belonging to one bin. This immediately gives an estimate of the errors of $\langle \bar{h}^n\rangle^c$, too. Another possible way is to measure the probability distribution $w(\bar{h}, \bar{h}+\Delta\bar{h})$ of the values of $\bar{h}$ during the updating. The expectation value of $\bar{h}^n$ is, obviously:

$$\langle \bar{h}^n\rangle = \sum_b \bar{h}_b^n w(\bar{h}_b, \bar{h}_b + \Delta\bar{h}_b) \tag{16}$$

Here the sum goes over the bins $(\bar{h}, \bar{h}+\Delta\bar{h})$ for the values of $\bar{h}$. Of course, this equation is exact only in the limit $\Delta\bar{h} \to 0$. The error estimate for $\langle \bar{h}^n\rangle^c$ is somewhat combersome in this case, because one has to consider subsets of the performed sweeps, and obtain the probability distribution w and the value of $\langle \bar{h}^n\rangle^c$ in these subsets.

2.3 Monte Carlo results on 8^4 at $\beta = 2.3$

In the Monte Carlo simulation at $\beta = 2.3$ we mainly investigated the immediate vicinity of the confinement-Higgs phase transition. In the present Section we discuss the results for the masses and couplings obtained on the 8^4 lattice. Some similar results on the 12^4 lattice were already published in Ref. [6], and the comparison of 8^4 and 12^4 from the point of view of the order of the phase transition will be the subject of the next Section. Most of the points in the coupling parameter space are at $\lambda = \infty$ and $\lambda = 1.0$, but we have also a few points at $\lambda = 0.1$.

The Monte Carlo calculation was performed by using the Metropolis method with 6 hits per gauge invariant variables in the actions in Eq. (3), respectively Eq. (5). From previous experience [4] we know, that at such β-values the inclusion of the gauge degrees of freedom is unnecessary. The site- and link-variables were updated in alternating sweeps in a randomly changing order. The acceptance rate was kept near 1/3 per hit. We always used the full SU(2) group on the links. The boundary conditions were periodic. The total number of double-sweeps was typically $(8-10)\cdot 10^4$ per point. The statistical errors were estimated by binning the data in bins of length 2^k $(k = 0, 1, 2, \ldots)$, and estimating the standard deviations from the bin averages. Right on top of the phase transition very long time correlations were observed (sometimes in the order of 10000 sweeps), therefore the error estimates did not always saturate with the increasing bin length. In these points the errors may be underestimated. Away from the phase transition the time correlations are considerably smaller and, therefore, the statistical error estimates are reliable.

The measured masses in the W-boson (am_W) and Higgs-boson (am_H) channels and some average quantities like the average link L, average ρ-link R, average plaquette P, average length ρ and average action per site s are collected in Table I. The definitions of the average quantities are

$$L = \langle \frac{1}{2} Tr\, V(x,\mu)\rangle \qquad R = \langle \frac{1}{2}\rho_{x+\hat{\mu}}\rho_x Tr\, V(x,\mu)\rangle$$

$$P = \langle 1 - \frac{1}{2} Tr\, V_P\rangle \qquad \rho = \langle \rho_x\rangle$$

$$s = 6\beta\langle 1 - \frac{1}{2}Tr\, V_P\rangle + \langle \rho_x^2 - 3\log\rho_x + \lambda(\rho_x^2-1)^2\rangle + 8\kappa\langle 1 - \frac{1}{2}\rho_{x+\hat{\mu}}\rho_x Tr\, V(x,\mu)\rangle \tag{17}$$

The correlations could always be determined up to the largest distance ($d_{max} = 4$), therefore mass estimates could be obtained from all distances by using the formula

$$am^{(d)} = \frac{1}{(d_{max}-d)} \log\left\{ \frac{C_d}{C_{d_{max}}} + \sqrt{\left(\frac{C_d}{C_{d_{max}}}\right)^2 - 1}\right\} \qquad (0 \le d < d_{max}) \tag{18}$$

where C_d is the correlation at distance d. Usually, $d = 2, 3$ gives already consistent results, that is, these distances are reasonably well dominated by the lowest state. At some points, for instance very near to the phase transition in the W-boson channels, $am^{(3)}$ was still definitely smaller than $am^{(2)}$.

In such cases the time extension of the 8^4 lattice is obviously too small for a good mass estimate. In any case, the masses in Table I can be taken as upper limits. From this point of view, the situation on the 12^4 lattice is much better, because there $am^{(d)}$ could be taken with $d_{max} = 6$.

Table I.

The W-boson mass (am_W) and Higgs-boson mass (am_H) in lattice units on 8^4 lattice at $\beta = 2.3$. The average quantities L, R, P, ρ and s are defined in Eq. (17). The statistical errors in the last numerals are given in parentheses.

λ	κ	am_W	am_H	L	R	P	ρ	s
∞	0.380	1.40(13)	1.35(14)	0.2325(2)		0.3930(1)		8.756(2)
∞	0.385	1.11(14)	0.68(7)	0.2403(4)		0.3922(1)		8.753(3)
∞	0.388	0.94(11)	0.55(4)	0.2455(6)		0.3915(2)		8.744(5)
∞	0.390	0.78(9)	0.45(5)	0.2504(6)		0.3907(2)		8.729(4)
∞	0.392	1.16(12)	0.45(4)	0.2574(10)		0.3894(3)		8.702(7)
∞	0.393	0.86(8)	0.36(4)	0.2601(10)		0.3889(2)		8.694(6)
∞	0.394	0.76(8)	0.33(3)	0.2638(10)		0.3882(5)		8.677(14)
∞	0.395	0.68(6)	0.32(3)	0.2690(12)		0.3871(6)		8.653(14)
∞	0.396	0.66(6)	0.39(4)	0.2741(13)		0.3858(4)		8.633(12)
∞	0.397	0.66(6)	0.39(4)	0.2787(11)		0.3849(6)		8.60(2)
∞	0.398	0.53(7)	0.41(3)	0.2863(10)		0.3833(3)		8.561(6)
∞	0.400	0.66(7)	0.54(7)	0.2933(7)		0.3822(2)		8.536(4)
∞	0.402	0.56(5)	0.56(7)	0.2992(6)		0.3814(1)		8.518(4)
∞	0.405	0.51(5)	0.91(10)	0.3071(4)		0.3804(1)		8.494(3)
∞	0.410	0.53(4)	0.82(7)	0.3214(3)		0.3784(1)		8.448(2)
1.0	0.3036	0.64(9)	0.32(3)	0.2576(16)	0.3585(25)	0.3871(3)	1.1254(6)	8.406(9)
1.0	0.3038	0.61(6)	0.29(3)	0.2701(18)	0.3780(29)	0.3847(3)	1.1301(7)	8.332(9)
1.0	0.3039	0.74(6)	0.33(3)	0.2666(18)	0.3724(29)	0.3857(4)	1.1288(7)	8.357(10)
1.0	0.3040	0.58(6)	0.33(3)	0.2720(20)	0.3809(31)	0.3845(3)	1.1309(7)	8.322(10)
1.0	0.3041	0.62(6)	0.31(3)	0.2678(21)	0.3743(33)	0.3855(3)	1.1293(8)	8.352(10)
1.0	0.3042	0.69(8)	0.31(3)	0.2727(21)	0.3821(33)	0.3846(3)	1.1312(8)	8.325(10)
1.0	0.3045	0.67(7)	0.46(4)	0.2790(13)	0.3921(21)	0.3831(3)	1.1336(5)	8.283(9)
1.0	0.3070	0.53(5)	0.68(4)	0.3015(8)	0.4283(13)	0.3798(2)	1.1428(3)	8.171(4)
0.1	0.194	0.55(5)	0.25(3)	0.2882(46)	0.683(13)	0.3809(5)	1.4245(39)	7.360(17)
0.1	0.196	0.53(5)	0.86(3)	0.3485(6)	0.8710(20)	0.3733(2)	1.4800(6)	7.059(4)
0.1	0.250	1.12(3)	2.14(6)	0.7475(2)	3.5955(18)	0.31235(4)	2.1778(3)	3.481(2)

The masses of, respectively, the W-boson and Higgs-boson are shown in Fig. 1A and 1B as a function of the link expectation value L. The figures show that the approximate universality observed in Ref. [4] is good within the considerably smaller errors of the present calculation, too. In particular, the universality is not worse in the Higgs-channel than in the W-channel, quite contrary to the weak coupling perturbation theoretic expectation. The only point where a deviation from universality of the Higgs-mass may be indicated by the data is at ($\lambda = 0.1$, $\kappa = 0.194$). This point, however, is in the region of the phase transition, where metastability can be observed (see next Section). Since the metastability is strongly volume dependent, such points are not characteristic to the infinite volume limit. (In the next Section we shall also see that the metastability effects mainly the Higgs-mass.)

The new data confirm the qualitative behaviour of the masses seen in Ref. [4]. The W-mass is large below the phase transition. Just below the phase transition and in the phase transition region itself it drops rapidly to a value about $am_W \simeq 0.5$ and stays practically constant, with a rather slow increase, above the phase transition. The Higgs-mass am_H is greater or equal than am_W in the Higgs-phase

(i. e. above the phase transition), and smaller than am_W in the confinement phase (i. e. below the phase transition). Inside the phase transition region am_H has a rather small value ($am_H \simeq 0.3$ on the 8^4 lattice). All these features are in good agreement with the recent findings of the Aachen-Graz group [8] at slightly different parameter values.

For some technical reasons, the zero momentum couplings were not determined in every point. We have only two points with full statistics for the n-Higgs couplings (nH; n=3,4,5,6) and for the Higgs-WW coupling (HWW). As discussed in Section 2, these quantities are, in general, difficult to calculate with an acceptable statistical error, because the extraction of the connected parts from the correlation functions involves a high degree of cancellation. From this point of view the HWW coupling is somewhat more favourable than the 3H coupling. The 4H and 5H couplings are, of course, even more difficult, and the 6H coupling is not measurable at all within our statistics.

The two points where the couplings were determined are (always with $\beta = 2.3$):

$$\text{point A}: \quad \lambda = 1.0, \quad \kappa = 0.307; \qquad\qquad \text{point B}: \quad \lambda = 0.1, \quad \kappa = 0.196; \tag{19}$$

We tried both methods for the extraction of the connected parts discussed in Section 2. The probability distribution w for the average values was collected in 10000 bins. The two ways gave for the couplings identical results within errors. The distributions of the averages ρ, L and R at point A are shown in Figs. 2A-2C. The results for the nH couplings $\Lambda_{nH}^{(j)}$ obtained by using the interpolating fields $h^{(j)}$, $(j = 1, 2, 3)$ in Eq. (6) are:

$$\mathrm{A}: \begin{cases} a^{-2}\Lambda_{3H}^{(1)} = -5.6 \pm 2.5 & a^{-4}\Lambda_{4H}^{(1)} = (2.9 \pm 1.6) \cdot 10^2 \quad a^{-6}\Lambda_{5H}^{(1)} = (-1.5 \pm 1.3) \cdot 10^4 \\ a^{-2}\Lambda_{3H}^{(2)} = -11.0 \pm 5.5 & a^{-4}\Lambda_{4H}^{(2)} = (9.8 \pm 4.7) \cdot 10^2 \quad a^{-6}\Lambda_{5H}^{(2)} = (-4.7 \pm 4.5) \cdot 10^4 \\ a^{-2}\Lambda_{3H}^{(3)} = -9.4 \pm 5.2 & a^{-4}\Lambda_{4H}^{(3)} = (9.4 \pm 4.5) \cdot 10^2 \quad a^{-6}\Lambda_{5H}^{(3)} = (-3.3 \pm 4.2) \cdot 10^4 \end{cases}$$

$$\mathrm{B}: \begin{cases} a^{-2}\Lambda_{3H}^{(1)} = -6.9 \pm 3.2 & a^{-4}\Lambda_{4H}^{(1)} = (4.3 \pm 1.9) \cdot 10^2 \quad a^{-6}\Lambda_{5H}^{(1)} = (-1.1 \pm 0.5) \cdot 10^5 \\ a^{-2}\Lambda_{3H}^{(2)} = -12.6 \pm 5.0 & a^{-4}\Lambda_{4H}^{(2)} = (8.5 \pm 2.7) \cdot 10^2 \quad a^{-6}\Lambda_{5H}^{(2)} = (-6.0 \pm 8.8) \cdot 10^4 \\ a^{-2}\Lambda_{3H}^{(3)} = -7.8 \pm 4.3 & a^{-4}\Lambda_{4H}^{(3)} = (5.0 \pm 2.6) \cdot 10^2 \quad a^{-6}\Lambda_{5H}^{(3)} = (-4.5 \pm 7.7) \cdot 10^4 \end{cases} \tag{20}$$

The errors are, unfortunately, still very large. The dependence on the choice of the interpolating field is reduced for the ratios defined in Eq. (10). For instance, for the 3H and 4H couplings we have:

$$\begin{aligned} &\mathrm{A}: \quad \rho_{(3)4\mathrm{H}}^{(1)} \simeq 28.9 \qquad \rho_{(3)4\mathrm{H}}^{(2)} \simeq 39.8 \qquad \rho_{(3)4\mathrm{H}}^{(3)} \simeq 47.6 \\ &\mathrm{B}: \quad \rho_{(3)4\mathrm{H}}^{(1)} \simeq 33.0 \qquad \rho_{(3)4\mathrm{H}}^{(2)} \simeq 29.0 \qquad \rho_{(3)4\mathrm{H}}^{(3)} \simeq 32.1 \end{aligned} \tag{21}$$

Let us remark that in a recent paper [9] the zero momentum renormalized ϕ^4 coupling in the one- and four-component ϕ^4 model was calculated from the probability distribution w of averages. The aim was to obtain an upper bound on the Higgs-boson mass. Since the Monte Carlo calculation in Ref. [9] has only a rather limited statistics (42000 sweeps on 4^4 and 14000 sweeps on 6^4 lattice), it seems to us that the quoted small errors are incorrect. (The way of estimating the errors is not discussed in the paper.)

The HWW coupling has smaller errors, and its dependence on the choice of $h^{(j)}$, $(j = 1, 2, 3)$ is negligible compared to the statistical errors, therefore we averaged this coupling over j. The influence of the choice of the interpolating field for the W-boson $w^{(k)}$, $(k = 1, 2)$ in Eq. (7) is more significant:

$$\mathrm{A}: \quad \mathrm{a}^{-2}\Lambda_{\mathrm{HWW}}^{(\mathrm{k=1})} = 1.66 \pm 0.28 \qquad \mathrm{a}^{-2}\Lambda_{\mathrm{HWW}}^{(\mathrm{k=2})} = 2.56 \pm 0.24$$

$$B: \quad a^{-2}\Lambda_{HWW}^{(k=1)} = 1.60 \pm 0.21 \qquad a^{-2}\Lambda_{HWW}^{(k=2)} = 3.34 \pm 0.27 \tag{22}$$

One can see that, within the present errors, the couplings show no dramatic λ-dependence.(Note that, according to Table I, the link expectation values are only approximately equal in the two points.) Of course, the large errors of the nH couplings, unfortunately, prevent any firm conclusions for the moment. A dedicated high statistics numerical study of the couplings clearly deserves future attention.

3 8^4 versus 12^4 lattice

3.1 Questionning the order of the phase transition

The order of the confinement-Higgs phase transition is an important issue in the standard SU(2) Higgs model. In particular, the existence and properties of the continuum limit at the $\beta = \infty$ critical points may depend also on the order of the phase transition at finite β. In the case of a second order phase transition line in the $\lambda = const.$ planes the correlation lengths are infinite along this line. This allows for the expected exponential rise of the correlation lengths $\exp(const.\beta)$ along the renormalization group trajectories (RGT's) going to the critical point at $\beta = \infty$ near the phase transition line. The picture of the RGT's in the (β, κ)-plane is then qualitatively given by Fig. 3A. In this case the analogy between the SU(2) gauge theory with scalar doublet matter field (for λ=fixed) and an SU(2) gauge theory with a spin-$\frac{1}{2}$ fermion doublet is almost perfect, since for fermions there is also a second order critical line at zero fermion mass. If, however, the phase transition line in the Higgs model is first order everywhere except for the endpoint at $\beta = \infty$ (where it is second order), then there is no reason for the correlation lengths to diverge for finite β. If the maximum of the correlation lengths does not increase sufficiently fast for $\beta \to \infty$, then the (approximate) RGT's can not reach the critical point at $\beta = \infty$: they end on the discontinuity at the first order line for some finite correlation length, as it is shown by Fig. 3B. In this case the critical point at $\beta = \infty$ is likely to be trivial (i.e. equivalent to the pure gauge theory in the confinement phase and to a free theory of massive bosons in the Higgs-phase). Therefore, in the case of a first order phase transition line, the sufficiently fast increase of the maximum correlation length along the line is a non-trivial requirement for the existence of a non-trivial continuum limit in the $\beta = \infty$ critical point.

Recent high statistics Monte Carlo results imply [8] that for small λ the confinement-Higgs phase transition is strongly first order. For increasing λ and/or increasing β it is observed that the first order transition becomes weaker. Therefore, in principle, it is possible that on the phase transition surface there is a tricritical line and beyond this the transition is second order. However, as far as the λ-dependence is concerned, this does not seem to happen for $\beta = 2.3$, because of the two-state signal observed on a 12^4 lattice [6]. In this Section we want to elaborate on the question of the two-state signal by presenting more details of the 12^4 calculation and also by comparing the behaviour near the phase transition on 8^4 and 12^4 lattices.

The investigation of the volume dependence is important, because a statement about the order is, in fact, a statement about the volume dependence for very large volumes. Mathematically speaking the distinction refers only to the infinite volume limit but, of course, the qualitatively different features normally set in on finite, but large enough, lattices. In the case of an expected first order phase transition, however, one has to be aware of the peculiar volume dependence implied by the metastability of the two phases. On a finite lattice the first order phase transition is "rounded-off" and there is a finite range of parameters (in our case, for fixed λ and β, a range of κ), where the system shows metastability and flips between the two phases during the Monte Carlo iteration. This, of course, implies long range correlations. For increasing volume the range of metastability in κ shrinks to zero and also moves towards the discontinuity point for infinite volume. (For a systematic approach of the description of finite size effects in phase transitions see the recent paper of Brezin and Zinn-Justin [10], where references to previous work can also be found.) As a consequence, the observation of long range correlations in a finite volume does not necessarily mean second order phase transition. In the case of a first order phase transition, for fixed parameter values which do not coincide with the discontinuity, the long range correlation disappears once the volume is large enough. At a second order phase transition the region of large correlation lengths has a finite limiting extent. In other words, for a first order phase transition there are strong finite size effects in the region of metastability. Therefore the metastability region has to be avoided if one wants to draw conclusions about the properties of the infinite volume system.

3.2 Two-state signals

The Monte Carlo calculation on the 12^4 lattice was performed in the same way as on 8^4 (the number of sweeps was $(8-12)\cdot 10^4$ per point). Some results on 12^4 were already published in Ref. [6], for instance the masses and some average quantities. A summary for the 12^4 lattice, similar to Table I, is given by Table II.

Table II.

Summary of the masses and average quantities obtained on 12^4 lattice at $\beta = 2.3$.

λ	κ	am_W	am_H	L	R	P	ρ	s
∞	0.390	1.26(6)	0.40(2)	0.2485(2)		0.39126(8)		8.744(2)
∞	0.392	0.82(6)	0.35(2)	0.2535(3)		0.39047(9)		8.729(2)
∞	0.394	0.70(8)	0.35(4)	0.2599(4)		0.38937(15)		8.706(4)
∞	0.395	0.73(6)	0.21(2)	0.2677(8)		0.3876(3)		8.664(7)
∞	0.396	0.47(3)	0.24(2)	0.2735(6)		0.3864(4)		8.629(9)
∞	0.397	0.31(4)	0.26(2)	0.2783(6)		0.3854(3)		8.610(8)
∞	0.398	0.45(4)	0.44(3)	0.2856(4)		0.38377(14)		8.570(4)
∞	0.400	0.48(2)	0.53(4)	0.2931(3)		0.38253(11)		8.544(4)
∞	0.410	0.51(2)	0.79(3)	0.3214(2)		0.37860(5)		8.450(2)
1.0	0.3020	1.18(23)	0.63(7)	0.2378(4)	0.3275(6)	0.39125(9)	1.1177(2)	8.520(3)
1.0	0.3041	0.53(4)	0.16(1)	0.2651(14)	0.3702(21)	0.3863(3)	1.1284(5)	8.373(10)
1.0	0.3042	0.52(5)	0.17(2)	0.2682(14)	0.3750(21)	0.3855(3)	1.1295(5)	8.352(8)
1.0	0.3045	0.40(3)	0.18(2)	0.2751(14)	0.3860(22)	0.3840(3)	1.1322(5)	8.304(9)
1.0	0.3050	0.39(3)	0.35(4)	0.2865(6)	0.4039(10)	0.3821(2)	1.1365(3)	8.244(4)
1.0	0.3070	0.50(3)	0.57(5)	0.3030(4)	0.4308(6)	0.37973(6)	1.1434(2)	8.167(2)
1.0	0.3100	0.52(3)	0.78(4)	0.3229(3)	0.4639(5)	0.37720(6)	1.1520(1)	8.076(2)

The main emphasis in the comparison of 8^4 to 12^4 lattice was put on the behaviour at the phase transition. A study of the time dependence of the average quantities during the updating revealed a clear signal of metastability in a narrow range of κ (in the order of $\Delta\kappa \simeq 10^{-3} - 10^{-4}$). The resulting two-peak structure of the distribution of the average plaquette was shown in Ref. [6]. The time dependence of the average plaquette at ($\lambda = 1.0$, $\kappa = 0.3041$) is given in Fig. 4A. One point in the figure represents the average of 200 sweeps, but this averaging is not essential, it was chosen mainly for the better optical presentation. Taking averages over less sweeps (say 50 or 100) gives the same qualitative picture, of course, with larger intrinsic fluctuations within a phase. The two-peak structure of the distribution can also be seen without averaging (the curves become even smoother because of the large number of entries). The two peaks show up also in other average quantities, like average link, average ρ-link, average length, average action etc. For another example, the time dependence and the distribution of the average link is shown in Figs. 4B-4C.

On the 8^4 lattice a similar behaviour can be seen near the phase transition at a slightly smaller κ. For instance, the time dependence and distribution of the average link in the point ($\lambda = 1.0$, $\kappa = 0.3038$) is shown by Figs. 5A-5B. Although the fluctuations in Fig. 5A make an optical impression similar to Fig. 4B, the more reliable representation in terms of the distribution in Fig. 5B implies that the two-state signal is weaker on the 8^4 lattice. (In fact, the appearence of several points in Table I close to each other in κ is the result of a long search for metastability.) Fig. 5B alone would certainly be inconclusive for the existence of two metastable states. Going to a smaller λ-value makes the search for metastability much easier. For instance, the distribution of the average link on the 8^4 lattice at ($\lambda = 0.1$, $\kappa = 0.194$) in Fig. 5C shows a bump at a low average link. In the time development there is a clear flip to the low value. In fact, we planned this point for the measurement of the couplings, and the metastability was for that purpose an unpleasant surprise. Fig. 5C also shows that the distance of the two peaks is substantially larger at $\lambda = 0.1$ than at $\lambda = 1.0$, that is, for small λ the region of metastability is extending in the average link variable. Therefore, near the phase transition one has to be careful about the judgement of λ-universality, because it can be better in the large volume limit than for a fixed, relatively small, volume. This may explain the "bad" $\lambda = 0.1$ point for the Higgs-mass in Fig. 1B.

The lesson from all this is that for the distinction of first versus second order phase transition one has to

- tune the coupling parameters very carefully;
- collect high statistics (in the range of 10^5 sweeps or more);
- use large lattices (with 10^4 sites or more).

In our opinion, the weaker two-state signal at $\lambda = \infty$ on the 12^4 lattice [6] can be expected to become stronger (and conclusive) on lattices like 16^4 or 20^4. Therefore, the confinement-Higgs phase transition is probably first order at $\beta = 2.3$ for every λ.

3.3 Volume dependence of the susceptibility

The critical behaviour near a phase transition can also be investigated by calculating the normalized susceptibility χ_L for different lattice sizes L. The definition of χ_L can be

$$\chi_L = \frac{\sum_y [\langle Tr V(x,\mu)\, Tr V(y,\mu)\rangle - \langle Tr V(x,\mu)\rangle\langle Tr V(y,\mu)\rangle]}{\langle [Tr V(x,\mu)]^2\rangle - \langle Tr V(x,\mu)\rangle^2} \tag{23}$$

Due to the lattice symmetries, this does not depend on x and μ. Another possible definition would be to sum in the numerator over the link directions, too, but as short checks in a few points showed, this does not change any of the qualitative features. Therefore, we used the above definition, which was easier to implement in our programs.

Following the ideas of finite size scaling [11], it is customary to fit the susceptibility χ_L on L^4 lattice by the form [12,13]

$$\chi_L = C\left\{L^{-\frac{2}{\nu}} + \lambda_2(\kappa - \kappa_L)^2\right\}^{2\nu-1} \tag{24}$$

Here κ_L is the position of the maximum of susceptibility on the L^4 lattice. (It is assumed here, for simplicity, that only the hopping parameter κ changes, the other two couplings λ and β are fixed.) Besides the critical exponent of the correlation length $\nu < \frac{1}{2}$ there are two arbitrary parameters C, λ_2, which provide a simple parametrization of an arbitrary scaling function.

The data for χ_L ($L = 8, 12$) are shown in Fig. 6. Besides χ_L an analogous quantity in the W-boson channel is also given, which is defined similarly to χ_L, only in Eq. (23) TrV is replaced everywhere by $Tr(\tau V)$. As one can see, the phase transition influences χ_L strongly, but the analogous quantity in the W-channel shows no appreciable structure. Obviously, the phase transition dynamics is dominated by the zero momentum mode in the Higgs-boson channel.

For the susceptibility χ_L not even a qualitative fit could be achieved by the form in Eq. (24). The reason is that the growth of the maximum between 8^4 and 12^4 would require a critical exponent $\nu \simeq \frac{2}{5}$ (this corresponds to the roughly linear rise of the maximum with L). For such values of ν, however, the above form cannot reproduce the general shape of the curves, which have a somewhat flat plateau near the maximum and a rather abrupt decrease. Another functional form we also tried was

$$\chi_L = C \left\{ L^{-\frac{4}{\nu}} + \lambda_4 (\kappa - \kappa_L)^4 \right\}^{\nu - 0.5} \tag{25}$$

This gives a somewhat better description if the asymmetric 8^4 points, farther away from the maximum, are omitted from the fit. The 8^4 curve shown on Fig. 6 belongs to ($C = 0.6$, $\nu = 0.41$, $\lambda_4 = 80$, $\kappa_8 = 0.3955$). This describes the central part of the 8^4 points well, but the best choice of $\kappa_{12} = 0.396$ fails to reproduce the 12^4 curve. (The χ^2 is about 100.) We were unable to find any better simple fit. We are aware of the fact that logarithmic deviations from the above simple forms are expected in dimension four [14], but we do not think that this could explain the observed large deviations. Therefore, our conclusion is that the finite size analysis does not agree with the shape of the susceptibility curves. This is consistent with our expectation that the confinement-Higgs phase transition at $\beta = 2.3$ is of first order for every λ. Nevertheless, we do not consider the finite size analysis alone decisive. The main argument in favour of the first order transition comes from the observation of the two-state signal.

Note that the authors of Ref. [13] also concluded from their finite size analysis that the phase transition is of first order. Their argument, however, was based mainly on the apparent lack of increase of the maximum between $L = 4$ and 5. Here one can see, on larger lattices and with much better statistics, that the situation is more subtle because the maximum does increase with L. Obviously, finite size scaling ideas are applicable, if at all, only to really large lattices and at the same time good statistics and a reasonable relative change in lattice size is required, in order to see some effect.

4 Weak physical gauge coupling

4.1 How to choose the bare parameters?

The lattice actions (1), (3) of the standard SU(2) Higgs model have three bare parameters. One of the three, namely the scalar self-coupling λ, seems to be irrelevant in the wide range $0.1 \leq \lambda \leq \infty$, at least as far as the limited accuracy of the present Monte Carlo data can tell. Therefore, the value of λ can be fixed for convenience, and only the two relevant parameters β, κ have to be tuned in order to describe different possible physical situations. One combination of the parameters has to be used for fixing the scale. In a numerical Monte Carlo calculation this must be chosen in such a way that the smallest mass in lattice units be of the order 0.1-1. For the remaining combination of parameters a good physical characterization is provided by the short range Coulomb potential. For $\beta = 2.3$ the coefficient of the Coulomb term in the potential is $\frac{3}{4}\alpha_{SU(2)} \simeq 0.2 - 0.3$ [4], which corresponds to a strong renormalized SU(2) coupling $g_{ren}^2 \equiv 4\pi\alpha_{SU(2)} \simeq 3 - 5$. In the standard SU(2) $\otimes$ U(1) electroweak theory the value of g_{ren}^2 is much smaller: at the scale of the W-boson mass it is $g_{ren}^2 \simeq 0.5$, corresponding to $\alpha_{SU(2)} \simeq 0.04$. In order to do a Monte Carlo calculation in this physically interesting region, one has to increase β by keeping am_W at the order of 0.1-1. (One should also stay within the Higgs-phase, according to the standard situation in SU(2) $\otimes$ U(1).) In view of $g_{ren}^{-2} = g^{-2} + o(1)$, a good first guess is to take $\beta \equiv 4g^{-2} = 8$ and then try to tune the hopping parameter κ in such a way that am_W and am_H be in the measurable range 0.1-1.

The Monte Carlo data in the region of strong renormalized gauge coupling show that in the Higgs-phase $\alpha_{SU(2)}$ decreases with increasing κ. At the same time the ratio of the Higgs-boson to W-boson mass increases, starting from a value of about 1 just above the phase transition. Therefore, at the physical SU(2) coupling the ratio m_H/m_W is expected to be well above 1. This is a potential difficulty for the numerical calculation, because a mass ratio of the order of 10 or more is difficult to control with the presently available computing capacities. A first check at $\lambda = 1$, $\beta = 8$ and $\kappa = 0.28 - 0.32$ on 10^4 lattice showed [5] that m_H/m_W is about 6, which is difficult but seems feasible.

In this Section we shall present and discuss the results of a high statistics Monte Carlo calculation at $\beta = 8$. For such a high β the inclusion of the gauge degrees of freedom is important, therefore we used the lattice action in Eq. (1). Otherwise the calculation was performed in the same way as at $\beta = 2.3$. The value of the scalar self-coupling was $\lambda = 1.0$. On a 10^4 lattice we have chosen the hopping parameter $\kappa = 0.30$ and performed about $5 \cdot 10^4$ full sweeps. We shall refer to this point as **point C** . The other point is at $\kappa = 0.28$, on 12^4 lattice, and has about $2 \cdot 10^5$ sweeps. This will be called **point D** . It turned out that, generally speaking, the numerical Monte Carlo calculation at high β is not very much more difficult than at $\beta = 2 - 3$. The relaxation behaviour of the scalar degrees of freedom is completely normal and is quite similar to the behaviour in the pure ϕ^4 model at $\beta = \infty$. There is some noticeable rigidity in the gauge degrees of freedom, manifested by a slow drift of expectation values at the scale of a few thousand sweeps, but the amplitude is small even in the long distance quantities (like large Wilson loops or long distance correlations). In short, the numerical Monte Carlo investigation of the standard electro-weak model in the physical range of weak gauge couplings is feasible.

Future Monte Carlo calculations will hopefully allow for some limited change of the lattice spacing, too. In order to follow some singled out renormalization group trajectory (RGT), one has to keep $\alpha_{SU(2)}$ (or m_H/m_W) fixed for decreasing am_W. If the qualitative picture of the RGT's is given by Fig. 3A, then the RGT goes first close to the phase transition and then it goes to $\beta = \infty$ almost parallel to the phase transition line. In this latter stage the massless RG equation gives a good description of the change of lattice spacing. In the lowest order approximation the lattice spacing a depends exponentially on β:

$$a\Lambda_{SU(2)} \simeq \exp\left(-\frac{12\pi^2}{43}\beta\right) \tag{26}$$

Here $\Lambda_{SU(2)}$ is the RG invariant Λ-parameter for SU(2). In case of Fig. 3B Eq. (26) can still be approximately valid, but then the lattice spacing has a non-zero minimum value, corresponding to the finite β where the singled out RGT ends. Taking, as a first approximation, the mass independent Eq. (26) down to $am_W \simeq 0.1 - 1$, we have at $\beta = 8$

$$m_W/\Lambda_{SU(2)} \simeq 10^8 - 10^9 \tag{27}$$

This tells that the infrared scale of the SU(2) gauge coupling, where $\alpha_{SU(2)}$ becomes $o(1)$, is far below the scale of the W-mass. The large ratio in Eq. (27) may seem unnatural. In any case, one would like to have an explanation for it.

If the qualitative picture of the RGT's is given by Fig. 3B, one can speculate that perhaps the large scale ratio in Eq. (27) is connected to the large ratio of the Planck-mass (M_{Pl}) to the W-mass: $M_{Pl}/m_W \simeq 10^{17}$. Namely, if the RGT's end on the first order discontinuity, then every RGT has a characteristic maximum correlation length and a corresponding value of $\alpha_{SU(2)}$ at the discontinuity. In this case it is conceivable that the RGT realized in nature belongs to a specific (small) initial value of $\alpha_{SU(2)}$ at the Planck scale and the corresponding maximum correlation length happens to be 10^{17}. This would explain both large ratios M_{Pl}/m_W and $m_W/\Lambda_{SU(2)}$ as a consequence of the exponential change of the scale with β.

4.2 Yukawa potential

In order to determine the static energy (in short, "potential") of an external SU(2) doublet charge pair, the Wilson-loop expectation values were calculated in both points at $\beta = 8$. The statistics for the Wilson-loops was collected in about 8000 sweeps in point C and about 30000 sweeps in point D. The results are summarized in Table III. The potential at lattice distance R was extracted from the Wilson-loops $W_{R,T}$ by fitting the T-dependence with two exponentials for $1 \leq T \leq 5$ on the 10^4, and for $2 \leq T \leq 6$ on the 12^4 lattice.

The shape of the potential is expected to be Yukawa-like, corresponding to the massive W-boson exchange. On our lattices the physical potential is, however, distorted by both finite lattice size and finite lattice spacing effects. Since we are in a region of small gauge coupling, these effects can presumably be described (and corrected for) by lowest order perturbation theory. Let us, therefore, briefly consider the Yukawa potential in lattice perturbation theory.

Table III.

The expectation values of the Wilson-loops $W_{R,T} = W_{T,R}$ in the two points C and D defined in the text. Entries below the main diagonal refer to the point C (10^4 lattice), the rest gives the result in point D (12^4 lattice). Statistical errors are given in parentheses.

	$T=1$	$T=2$	$T=3$	$T=4$	$T=5$	$T=6$
$R=1$	0.90401(1)	0.83894(2)	0.78215(3)	0.72991(4)	0.68135(4)	0.63608(5)
$R=2,1$	0.90432(2)	0.75448(4)	0.68797(5)	0.62942(6)	0.57643(7)	0.52812(8)
$R=3,2$	0.83960(5)	0.75577(9)	0.62033(7)	0.56290(8)	0.51181(9)	0.46580(10)
$R=4,3$	0.78311(7)	0.68984(13)	0.62301(16)	0.50827(10)	0.46043(12)	0.41776(13)
$R=5,4$	0.73116(8)	0.63179(14)	0.56626(19)	0.51247(23)	0.41608(14)	0.37687(16)
$R=6,5$	0.68286(9)	0.57925(16)	0.51583(21)	0.46546(26)	0.42211(32)	0.34107(17)

The Yukawa potential in the continuum is generated by the exchange of a massive boson and is proportional to the integral

$$I(r,m) = \int \frac{d^3k}{(2\pi)^3} \frac{e^{i\mathbf{kr}}}{k^2+m^2} = \frac{1}{4\pi r} e^{-mr} \tag{28}$$

with $r \equiv |\mathbf{r}|$. A lattice version is given by

$$I(r,m,a) = \int_{-\pi/a}^{\pi/a} \frac{d^3k}{(2\pi)^3} \frac{e^{i\mathbf{kr}}}{\hat{k}^2+m^2} \tag{29}$$

where

$$\hat{k}_\mu = \frac{2}{a} \sin \frac{k_\mu a}{2} \tag{30}$$

Note that if aM is the mass determined by the decay of a 2-point function, then in the propagator one has $am = 2\sinh\frac{aM}{2}$. If we consider the Wilson-loop in perturbation theory and give the vector boson a mass, then in lowest order we obtain (for SU(N))

$$V(r) = -\lim_{T\to\infty} \frac{1}{aT} \log W_{R,T} = g^2 \frac{N^2-1}{2N} \int_{-\pi/a}^{\pi/a} \frac{d^3k}{(2\pi)^3} \left(1 - e^{ik_3 r}\right) \frac{1}{\hat{k}^2+m^2} + o(g^4)$$

$$= const. - \alpha_0 \cdot 4\pi \frac{N^2-1}{2N} I(r,m,a) + o(g^4) = const. - \alpha_0 \cdot 3\pi I(r,m,a) + o(g^4) \tag{31}$$

Here we used $R \equiv r/a$; $\alpha_0 \equiv g^2/(4\pi)$, and in the last step we have put $N=2$. The integral in Eq. (29) refers to the infinite volume limit. The deviations from the continuum integral give finite a effects. For small a we have, keeping m, r fixed

$$I(r,m,a) = \frac{1}{4\pi r} e^{-mr} \left\{ 1 + \frac{a^2}{4r^2} \left[1 + mr + \frac{(mr)^3}{6} \right] + o(a^4) \right\} \tag{32}$$

In our case we have relatively small volumes and large loops, therefore we expect significant finite volume effects. To get an estimate of such effects we consider a finite volume version of $I(r,m,a)$ (with $l \equiv aL$ as the physical lattice extension):

$$aI(r,m,a,l) \equiv J(\mu,R,L) = \frac{1}{L^3} \sum_{\mathbf{p}\neq 0} \frac{e^{ip_3 R}}{\mu^2 + \sum_i 4\sin^2\frac{p_i}{2}} \tag{33}$$

Here we have put $\mu = am$, and the sum goes over the vectors $\mathbf{p}$

$$p_i = \frac{2\pi n_i}{L}; \qquad n_i = 0, \ldots, L-1 \tag{34}$$

The difference of sums $J'(\mu, R, L) \equiv J(\mu, R-1, L) - J(\mu, R, L)$ for $(\mu = 0.19,\ L = 12)$, respectively, $(\mu = 0.24,\ L = 10)$ is given in Table IV. One can see that for the larger R-values the finite volume effects are sizeable. The dependence on μ is small in this range.

Table IV.

The finite size dependence of $J'(\mu, R, L)$ for a few characteristic parameter values.

R	$\mu = 0.19, L = 12$	$\mu = 0.19, L = 20$	$\mu = 0.19, L = \infty$	$\mu = 0.24, L = 10$	$\mu = 0.24, L = \infty$
2	4.168E-2	4.170E-2	4.171E-2	4.088E-2	4.114E-2
3	1.393E-2	1.410E-2	1.412E-2	1.315E-2	1.369E-2
4	5.795E-3	6.174E-3	6.209E-3	4.910E-3	5.871E-3
5	2.551E-3	3.224E-3	3.275E-3	1.320E-3	3.009E-3
6	7.389E-4	1.861E-3	1.931E-3		

We define an effective SU(2) gauge coupling on our lattices by

$$\alpha_{SU(2)} \equiv \frac{a}{3\pi} \frac{V(aR) - V(aR - a)}{J'(\mu, R, L)} \tag{35}$$

From the Monte Carlo data in Table III we obtain, in point C with $(\mu = 0.24,\ L = 10)$ for distances $R = 2, 3$, respectively:

$$C: \qquad \alpha_{SU(2)} = 0.0478(5),\ 0.051(4) \tag{36}$$

This is somewhat larger than the value reported in Ref. [5], because there just a simple Coulomb-form was assumed for the short distance potential. In point D with $(\mu = 0.19,\ L = 12)$, for distances $R = 2, 3, 4$, we get

$$D: \qquad \alpha_{SU(2)} = 0.0476(2),\ 0.0496(12),\ 0.051(7) \tag{37}$$

These are remarkably consistent with R-independence and not far from the naive value $g^2/(4\pi) \simeq 0.040$. One can also see that, within our errors, there is no difference between the points C and D. From the data at strong gauge coupling it is expected that the exact value should be slightly smaller in point C than in point D.

4.3 Mass ratios and zero momentum couplings

For the determination of masses and zero momentum couplings the same quantities were calculated as in the 8^4 points discussed in Section 2. A summary for the $\beta = 8$ points C and D (defined above), similar to Table I-II, is given in Table V.

Table V.

Summary of the masses and average quantities in the two points C and D at $\beta = 8.0$.

λ	κ	am_W	am_H	L	R	P	ρ	s
1.0	0.30	0.24(2)	1.39(12)	0.4652(2)	0.7048(2)	0.09568(1)	1.2004(1)	6.9214(6)
1.0	0.28	0.19(1)	1.21(8)	0.3695(1)	0.5295(1)	0.09598(1)	1.1560(1)	7.2027(2)

The extraction of the mass in the W-boson channel is straightforward but in the Higgs channel one has to be careful, because the two-W states can also appear. Since on the larger lattice (12^4) we have much better statistics, we shall discuss point D in detail and give only the final results in the 10^4 point C.

The zero momentum correlations $C_w^{(k)}$ obtained by the interpolating fields $w^{(k)}$ in Eq. (7) are strongly dominated by a single low mass state. The distances $3 \leq d \leq 6$ can be well fitted by a single exponential:

$$C_w^{(1)}(d) = (0.128 \pm 0.011) \exp\{-d(0.196 \pm 0.016)\} + (d \to 12 - d)$$
$$C_w^{(2)}(d) = (0.133 \pm 0.013) \exp\{-d(0.196 \pm 0.018)\} + (d \to 12 - d) \qquad (38)$$

The correlations are always normalized by the value of the zero momentum correlation at distance zero. (The sum of the zero momentum correlation over the timeslices gives the susceptibility analogous to χ_L in Eq. (23).) The correlations $C_w^{(k)}$ can be well fitted by a single mass also for distances $2 \leq d \leq 6$, but then the masses are 5-10% higher. This shows that the excited states in the W-channel have either very high mass or are weakly coupled. A two-mass fit for $1 \leq d \leq 6$ is consistent with a second state about 10-12-times heavier than the lowest state. The $3 \leq d \leq 6$ fits in the lowest non-zero momentum channel give:

$$\tilde{C}_w^{(1)}(d) = (0.076 \pm 0.002) \exp\left\{-d\sqrt{\frac{\pi^2}{36} + (0.183 \pm 0.019)^2}\right\} + (d \to 12 - d)$$

$$\tilde{C}_w^{(2)}(d) = (0.079 \pm 0.002) \exp\left\{-d\sqrt{\frac{\pi^2}{36} + (0.185 \pm 0.020)^2}\right\} + (d \to 12 - d) \qquad (39)$$

The mass obtained from $\tilde{C}_w^{(k)}$ is practically the same as the one from $C_w^{(k)}$, therefore Lorentz invariance is well satisfied. The result for the W-boson mass, together with point C, is

$$C: \quad am_W = 0.24(2); \qquad D: \quad am_W = 0.19(1); \qquad (40)$$

The correlations $C_h^{(j)}$ of the variables in Eq. (6) have a qualitatively different behaviour, because there are clearly at least two masses present. This is shown by a fast decrease at smaller distances and a strong flattening-off at the largest distances. The statistical errors are, unfortunately, still somewhat too large, especially in the correlations of $h^{(1)}$, therefore we shall here consider only $C_h^{(j)}$, $(j = 2, 3)$. Two mass fits for the distances $1 \leq d \leq 6$ are:

$$C_h^{(2)}(d) = (1.17 \pm 0.02)\{(0.008 \pm 0.005) \exp\{-d(0.27 \pm 0.11)\} + \exp\{-d(1.24 \pm 0.08)\}\} + (d \to 12 - d)$$
$$C_h^{(3)}(d) = (1.50 \pm 0.06)\{(0.018 \pm 0.012) \exp\{-d(0.42 \pm 0.14)\} + \exp\{-d(1.24 \pm 0.12)\}\} + (d \to 12 - d) \qquad (41)$$

This shows that there is a strongly coupled high mass state and a very weakly coupled low mass state with a coupling strength of about only 1%. (Correspondingly, the low mass is badly determined.) The mass of the lower state is consistent, within large errors, with twice the W-mass, therefore we interpret it as 2W state with relative momentum zero. This interpretation is supported by the comparison to the low-β results. Namely, the correlations in the low-β points with $m_H \simeq 2m_W$ look qualitatively different. By fixing the low mass at $2am_W = 0.38$, it becomes possible to obtain a stable fit for $2 \leq d \leq 6$:

$$C_h^{(2)}(d) = (1.15 \pm 0.12)\{(0.015 \pm 0.008) \exp\{-d0.38\} + \exp\{-d(1.22 \pm 0.07)\}\} + (d \to 12 - d)$$

$$C_h^{(3)}(d) = (1.45 \pm 0.16)\{(0.013 \pm 0.008) \exp\{-d0.38\} + \exp\{-d(1.20 \pm 0.08)\}\} + (d \to 12 - d) \quad (42)$$

This is nicely consistent with the two mass fit in Eq (41), showing the dominance of a single high mass state already for $d = 1$. Therefore we conclude:

$$C: \quad am_H = 1.39(12); \qquad D: \quad am_H = 1.21(8); \qquad (43)$$

In point C the two mass fit is not possible due to the larger errors, nevertheless the flattening-off at the largest distances can still be seen. The value in point C in Eq. (43) was obtained from the distances $1 \leq d \leq 3$. (In point D the distances $1 \leq d \leq 3$ give a mass consistent with Eq. (43).)

If our interpretation of the states in the Higgs-boson channel is correct, then besides the zero relative momentum 2W-state there are also other states to be expected below the high mass Higgs-boson resonance, namely zero relative momentum multi-W states and also multi-W states with non-zero relative momentum. The resolution of all these states is impossible on our lattice even if higher statistical accuracy would be available. One can expect, however, that the multi-W states are all weakly coupled, similarly to the observed low mass state, therefore cannot be responsible for the dominant high mass state. In future Monte Carlo calculations one has to study the volume dependence of the spectrum on lattices elongated in time, which allow for the better separation of several exponentials. For the theoretical background to the volume dependence of the multi-particle spectrum, including resonances, see Ref. [15].

The zero momentum couplings were measured in the same way as for $\beta = 2.3$. Since in the continuum limit the Higgs couplings are expected to be induced by the gauge coupling, here we expect in general smaller couplings. These are, of course, even more difficult to calculate with sufficient precision than the relatively strong couplings at $\beta = 2.3$. In point C the nH couplings disappear completely in the noise. The only useful information we could obtain was for the HWW coupling:

$$\mathrm{C}: \quad \mathrm{a}^{-2}\Lambda^{(k=1)}_{\mathrm{HWW}} = 1.56 \pm 0.42 \qquad \mathrm{a}^{-2}\Lambda^{(k=2)}_{\mathrm{HWW}} = 2.29 \pm 0.41 \tag{44}$$

In point D the situation is slightly better: at least some information for the 3H and 4H couplings could be obtained:

$$\mathrm{D}: \qquad \mathrm{l}_{3\mathrm{H}} = -6.2 \pm 2.8; \qquad \mathrm{m}_{\mathrm{W}}^{4/3}\rho_{(3)4\mathrm{H}} \leq 5 \tag{45}$$

For the HWW coupling the result in point D is:

$$\mathrm{D}: \quad \mathrm{a}^{-2}\Lambda^{(k=1)}_{\mathrm{HWW}} = 0.79 \pm 0.32 \qquad \mathrm{a}^{-2}\Lambda^{(k=2)}_{\mathrm{HWW}} = 1.54 \pm 0.35 \tag{46}$$

This corresponds to an average value $l_{HWW} \equiv m_H m_W \Lambda_{HWW} = 0.27(10)$, substantially smaller than the value obtained from the tree level relation $l_{HWW} = g_{ren} \simeq 0.8$. Assuming pole dominance of the zero momentum HWW amplitude, the 2W width Γ_{HWW} of the Higgs-boson is given by

$$\frac{\Gamma_{HWW}}{m_H} = \frac{3m_H^2}{128\pi m_W^2} l_{HWW}^2 \sqrt{1 - \frac{4m_W^2}{m_H^2}} \left(1 - \frac{4m_W^2}{m_H^2} + \frac{12m_W^4}{m_H^4}\right) \simeq 0.019 \tag{47}$$

For a Higgs-boson mass of $m_H \simeq 500$ GeV our value of l_{HWW} gives a width of about 10 GeV.

5 Concluding remarks

Let us briefly summarize the main results of the Monte Carlo calculation:

- The approximate λ-independence of the W-boson and Higgs-boson mass, if considered as a function of the link expectation value, turned out to be valid within the present statistical errors (see Figs. 1A-1B and also the corresponding Figs. 2A-2B for 12^4 in Ref. [6]).

- The detailed study of the behaviour near the confinement-Higgs phase transition at $\beta = 2.3$ revealed strong indications of metastability at $\lambda = 1.0$ and a somewhat weaker two-state signal at $\lambda = \infty$ (see also Ref. [6]). The comparison of the susceptibility on 8^4 and 12^4 lattices is not consistent with simple finite size scaling. Therefore, the long range Higgs-channel correlations on finite lattices in the phase transition region are presumably due to the metastability associated to first order and not to the critical behaviour associated to second order phase transition. Our conclusion is that the confinement-Higgs phase transition is probably first order for every λ at finite β.

- The zero momentum n-Higgs-boson couplings are numerically difficult to obtain. Because of the large statistical errors the present results can only be considered as upper limits in absolute value. The zero momentum Higgs-WW coupling turned out to be measurable and does not show strong λ-dependence between $\lambda = 1.0$ and $\lambda = 0.1$.

- A high statistics Monte Carlo calculation at weak physical gauge coupling, roughly equal to the weak SU(2) coupling in the standard SU(2) $\otimes$ U(1) electro-weak theory, showed that a numerical investigation is feasible also in this region of couplings. The chosen value $\lambda = 1.0$ of the scalar self-coupling is in the non-perturbative range, where the non-perturbative feature of λ-independence is expected. (In fact, the observed λ-independence at $\beta = 2.3$ and $\beta = \infty$ strongly suggests a similar λ-independence at $\beta = 8$, too.) The main questions which can be answered in a Monte Carlo calculation are: the Higgs-boson to W-boson mass ratio, multi-Higgs and Higgs-W couplings etc. The $2 \cdot 10^5$ sweeps on a 12^4 lattice allowed the separation of two distinct states in the Higgs-boson channel: a weakly coupled state with roughly twice the W-mass and a strongly coupled high mass state with

$$\frac{m_H}{m_W} = 6.4 \pm 0.8 \tag{48}$$

  Our interpretation for the low mass state, based on the comparison to the low-β points, is that it is a zero relative momentum 2W-state, therefore the Higgs-W mass ratio is as given by Eq. (48). However, at present we cannot exclude the possibility $m_H/m_W \simeq 2$. (Future careful studies of the volume dependence of the spectrum may distinguish between the two possibilities.) The W-boson channel is dominated by the lowest state. The next excited W-state has a 10-12-times higher mass. For the n-Higgs couplings we only obtained upper bounds in absolute value, but the zero momentum Higgs-WW coupling turned out to be measurable. Its value is roughly by a factor of 3 smaller than the naive application of the tree-level formulas would give. Therefore, the width of the high mass Higgs-boson can be reasonably small, unless decays into multi-W channels dominate.

Our present understanding of the standard SU(2) Higgs model in the weak gauge coupling region can be considerably improved with an acceptable amount of computing time. In particular, one should study the λ-dependence, the volume dependence and, last but not least, the renormalization group properties. An important step would be to push the Monte Carlo calculation (for fixed β) towards the small-λ perturbative regime. As already mentioned in the introduction, the present numerical calculations of masses, couplings and other physical quantities are in the non-perturbative region of approximate λ-independence, corresponding to an effectively strong scalar self-coupling. (Therefore, assuming a monotonous λ-dependence for small λ, Eq. (48) can also be considered as an upper bound.) It is an interesting question where, for a given finite β, the perturbative behaviour in λ sets in. This is numerically non-trivial because the Monte Carlo calculation of physical quantities seems difficult for very small λ. The reason is the flat effective potential for the Higgs-field length and the corresponding ineffectiveness of the Monte Carlo process to probe a representative sample of configurations. We think, however, that also this difficulty can be overcome, perhaps by some more efficient Monte Carlo procedure. Taking all the foreseeable difficulties into account, we believe that a Monte Carlo calculation of the Higgs-boson mass with 10% error is easier in the standard SU(2) $\otimes$ U(1) model than the Monte Carlo calculation of the proton mass in QCD with 1% accuracy.

In order to have a firm theoretical interpretation of the Monte Carlo data, one has also to do more analytic work. The numerical calculation is necessarily restricted to relatively small cut-off's. The extension of the conclusions to higher cut-off's requires that numerical calculations be performed also in the validity range of an analytic expansion. In particular, a small gauge coupling expansion around the critical line $\kappa_{cr}(\lambda)$ (λ fixed) of the ϕ^4 model at $\beta = \infty$ should be done [16].

All our Monte Carlo data are consistent with the expectation that the pattern of the RGT's is given either by Fig. 3A or by Fig. 3B. The first would be the case if the confinement-Higgs phase transition would be second order, or if the maximum correlation length at the first order transition would increase sufficiently fast for $\beta \to \infty$. This would imply the existence of a non-trivial true continuum limit, in the mathematical sense, at the $\beta = \infty$ critical point. In the second case no exact continuum limit would exist, suggesting a fundamental difference between elementary fermion and scalar matter fields. Due to the bounded correlation length at the first order phase transition, the RGT's would end on the discontinuity for finite lattice spacing (i. e. for finite cut-off). Of course, if the maximum cut-off would be very high, the distinction would not be important from the practical point of view. Moreover, as we argued in Section 4, identifying the maximum cut-off with the scale of quantum gravity could provide a natural explanation for the observed large scale ratios M_{Pl}/m_W and $m_W/\Lambda_{SU(2)}$.

Acknowledgement

We are indebted to W. Hollik, M. Lüscher and T. T. Wu for helpful discussions.

References

[1] K. G. Wilson, Phys. Rev. **D10** (1974) 2445.

[2] for a review see, for instance, J. Fröhlich, in *Progress in gauge field theory,* Cargèse lecture 1983, ed. G. 't Hooft et al., Plenum Press 1984; for further references see this paper and also Ref. [4].

[3] J. Jersák, talk given at the Wuppertal Workshop on Lattice Gauge Theory, November 1985, to be published in the Proceedings.

[4] I. Montvay, *Correlations and static energies in the standard Higgs model,* DESY preprint 85-005 (1985), to be published in Nucl. Phys. B; for a discussion see also Ref. [5].

[5] I. Montvay, *The standard Higgs model on the lattice,* DESY preprint 85-050 (1985), to be published in the Proceedings of the conference "Advances in Lattice Gauge Theory", April 1985, Tallahassee, Florida

[6] W. Langguth, I. Montvay, *Two-state signal at the confinement-Higgs phase transition in the standard SU(2) Higgs model,* DESY preprint 85-094 (1985), to be published in Phys. Lett. B.

[7] D. J. E. Callaway, R. Petronzio, *Can elementary scalar particles exist?,* CERN-TH 4270/85 preprint (1985).

[8] J. Jersák, C. B. Lang, T. Neuhaus, G. Vones, *Properties of phase transitions of the lattice SU(2) Higgs model,* Aachen preprint PITHA 85/05 (1985).

[9] M. M. Tsypin, *The effective potential of lattice ϕ^4 theory and the upper bound on the Higgs mass,* Lebedev Institute, Moscow preprint, no. 280 (1985).

[10] E. Brezin, J. Zinn-Justin, Nucl. Phys. **B257** [**FS14**] (1985) 867.

[11] M. E. Fisher, in *Critical phenomena, Proceedings of the 51st Enrico Fermi Summer School,* Varenna 1970, ed. M. S. Green, Academic Press, New York 1972;
for a recent review see: M. N. Barber, in *Phase transitions and critical phenomena,* vol. VIII., ed. C. Domb, J. Lebowitz, Academic Press, New York, 1984.

[12] B. Lautrup, M. Nauenberg, Phys. Lett. **95B** (1980) 63.

[13] M. Tomiya, T. Hattori, Phys. Lett. **140B** (1984) 370.

[14] E.Brezin, Journ. Physique **43** (1982) 15.

[15] M. Lüscher, in preparation.

[16] I. Montvay, in preparation.

Figure captions

Fig. 1A. The W-boson mass in lattice units (am_W) as a function of the link expectation value $L = \langle \frac{1}{2} Tr\, V(x,\mu) \rangle$ for different λ-values at $\beta = 2.3$, on 8^4 lattice.

Fig. 1B. The same as Fig. 1A, for the Higgs-boson mass (am_H).

Fig. 2A. The distribution of average field length (ρ) in the point ($\lambda = 1$, $\beta = 2.3$, $\kappa = 0.307$) during the updating.

Fig. 2B. The same as Fig. 2A for the average link (L).

Fig. 2C. The same as Fig. 2A for the average ρ-link (R) defined in Eq. (17).

Fig. 3A. The schematic picture of RGT's in a $\lambda = const.$ plane in the case of a second order phase transition line (full line). The dashed-dotted lines are the RGT's in the Higgs-phase, the dashed ones the RGT's in the confinement phase. The correlation lengths diverge for $\beta \to \infty$.

Fig. 3B. The same as Fig. 3A in the case of a first order phase transition line (full line) ending in a second order point $\beta = \infty, \kappa_{cr}(\lambda)$, provided that the correlation length along the phase transition line is not increasing fast enough for $\beta \to \infty$.

Fig. 4A. The time dependence of average plaquette on a 12^4 lattice at ($\lambda = 1.0$, $\beta = 2.3$, $\kappa = 0.3041$). One point represents the average of 200 consequtive sweeps.

Fig. 4B. The time dependence of average link on a 12^4 lattice at ($\lambda = 1.0$, $\beta = 2.3$, $\kappa = 0.3041$). One point represents the average of 200 consequtive sweeps.

Fig. 4C. The distribution of the points in Fig. 4B.

Fig. 5A. The time dependence of average link on a 8^4 lattice at ($\lambda = 1.0$, $\beta = 2.3$, $\kappa = 0.3038$). One point represents the average of 200 consequtive sweeps.

Fig. 5B. The distribution of the points in Fig. 5A.

Fig. 5C. The distribution of average link on a 8^4 lattice at ($\lambda = 0.1$, $\beta = 2.3$, $\kappa = 0.194$). One entry represents the average of 200 consequtive sweeps.

Fig. 6. The susceptibility χ_L, defined in Eq. (23), for $L = 8, 12$. The curves give the best finite size scaling fit we could achieve with the form in Eq. (25) (see text). The squares represent an analogous quantity τ_L in the W-boson channel, which is defined like χ_L in Eq. (23), only TrV is replaced everywhere by $Tr(V\tau)$.

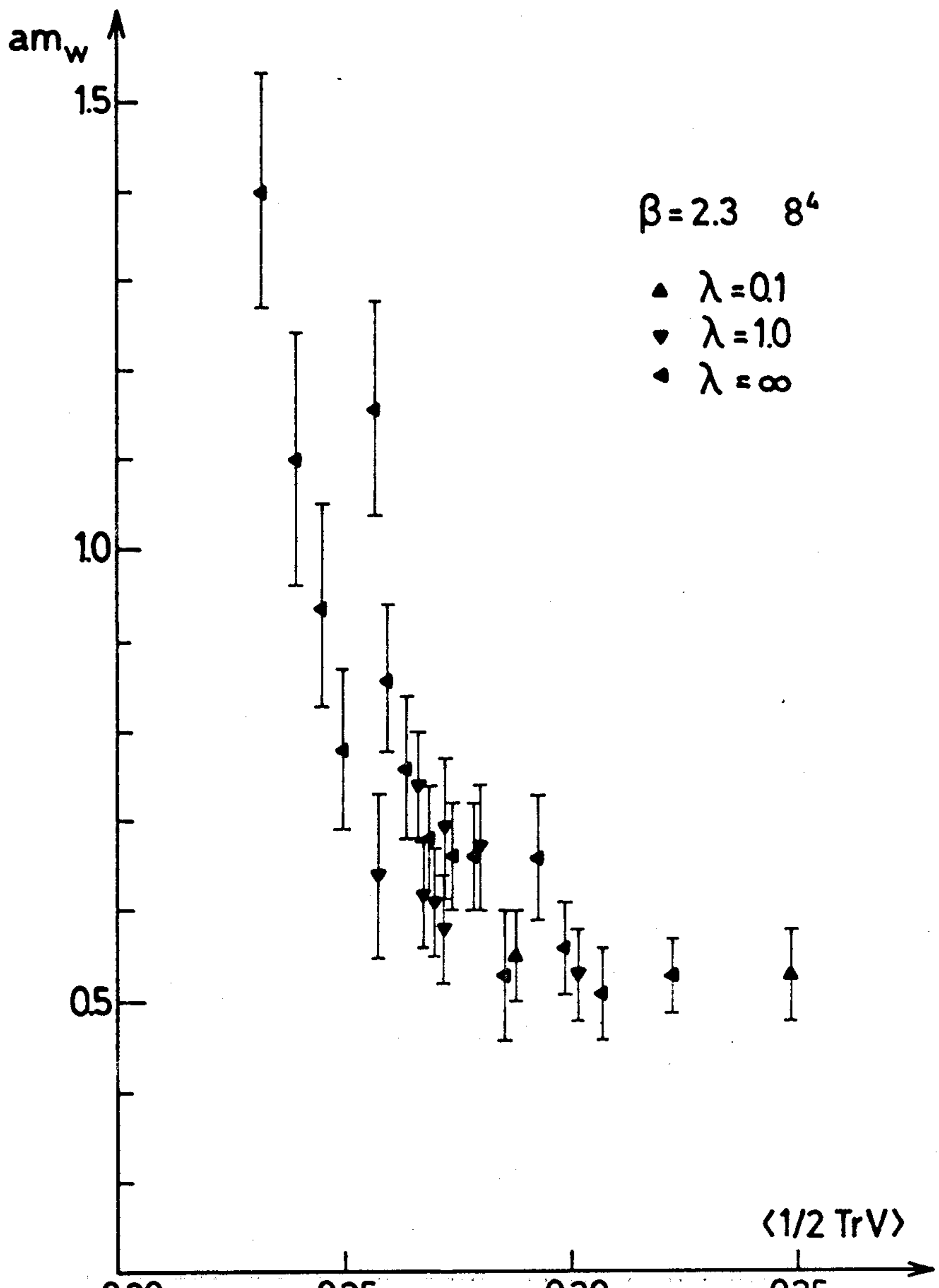

am_W
1.5
1.0
0.5
$\beta = 2.3 \quad 8^4$
$\lambda = 0.1$
$\lambda = 1.0$
$\lambda = \infty$
⟨1/2 TrV⟩
0.20
0.25
0.30
0.35

Fig. 1a

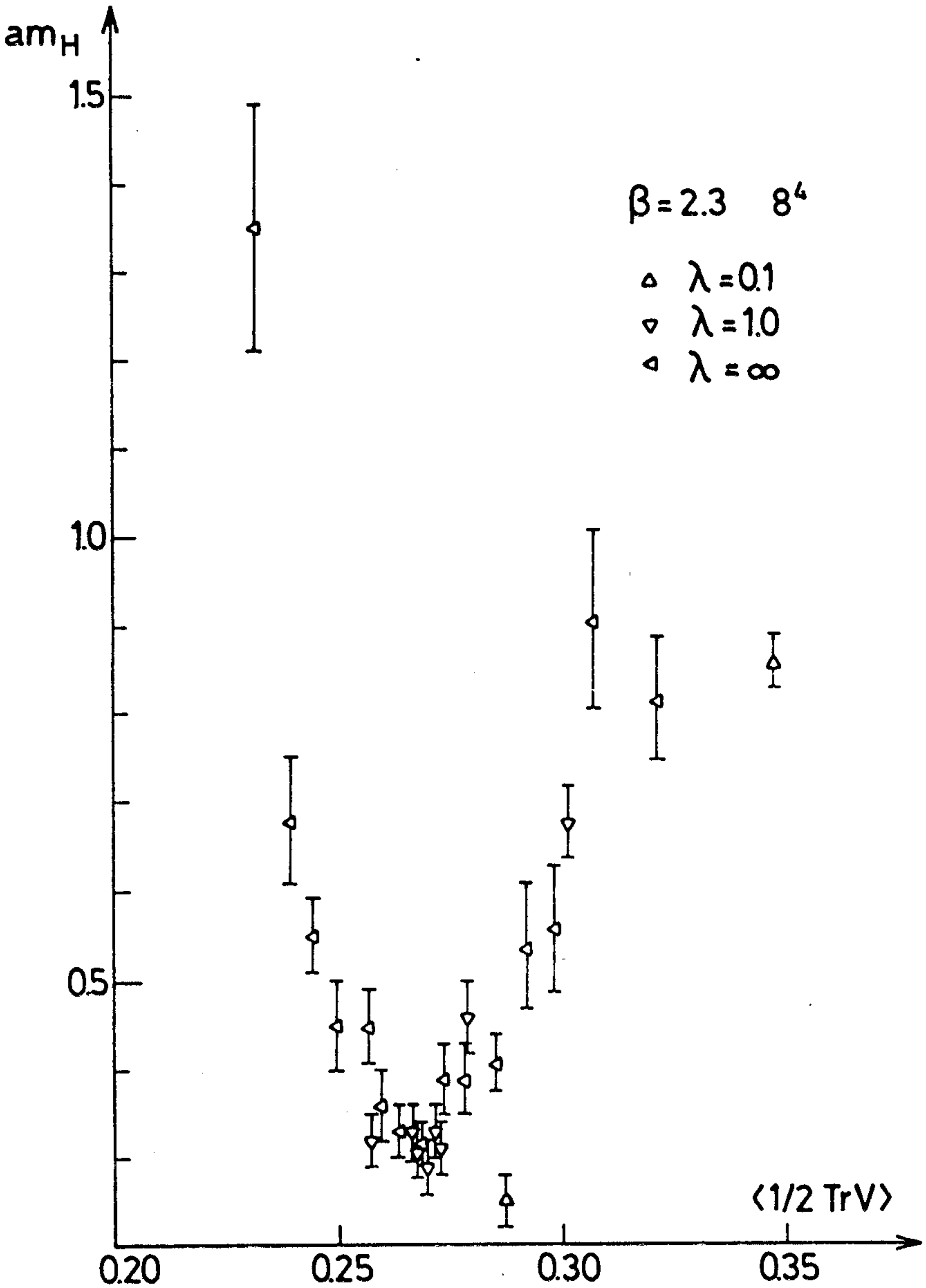

am_H
1.5
1.0
0.5
$\beta = 2.3 \quad 8^4$
$\lambda = 0.1$
$\lambda = 1.0$
$\lambda = \infty$
⟨1/2 TrV⟩
0.20
0.25
0.30
0.35

Fig.1b

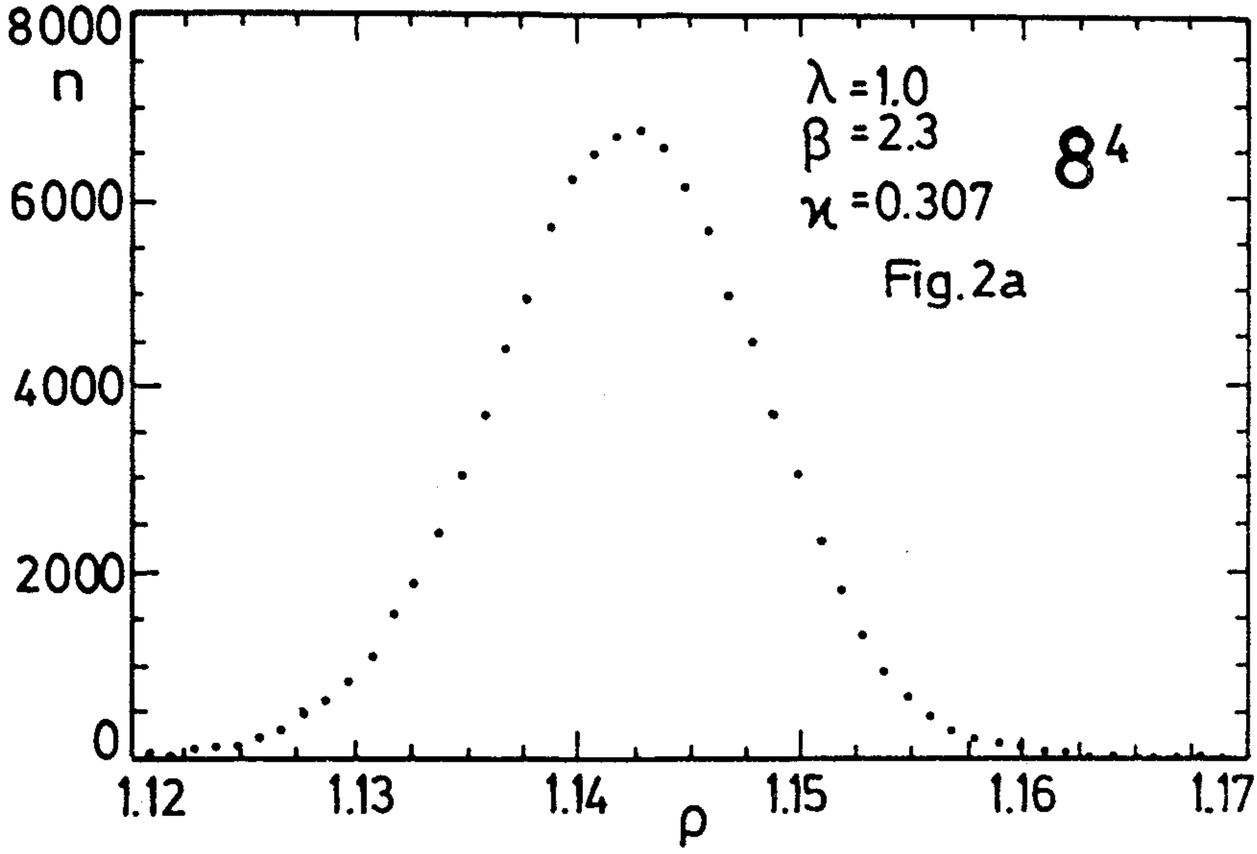
8000
n
6000
4000
2000
0
1.12
1.13
1.14
1.15
1.16
1.17
ρ
λ =1.0
β =2.3
ϰ =0.307
8⁴
Fig. 2a

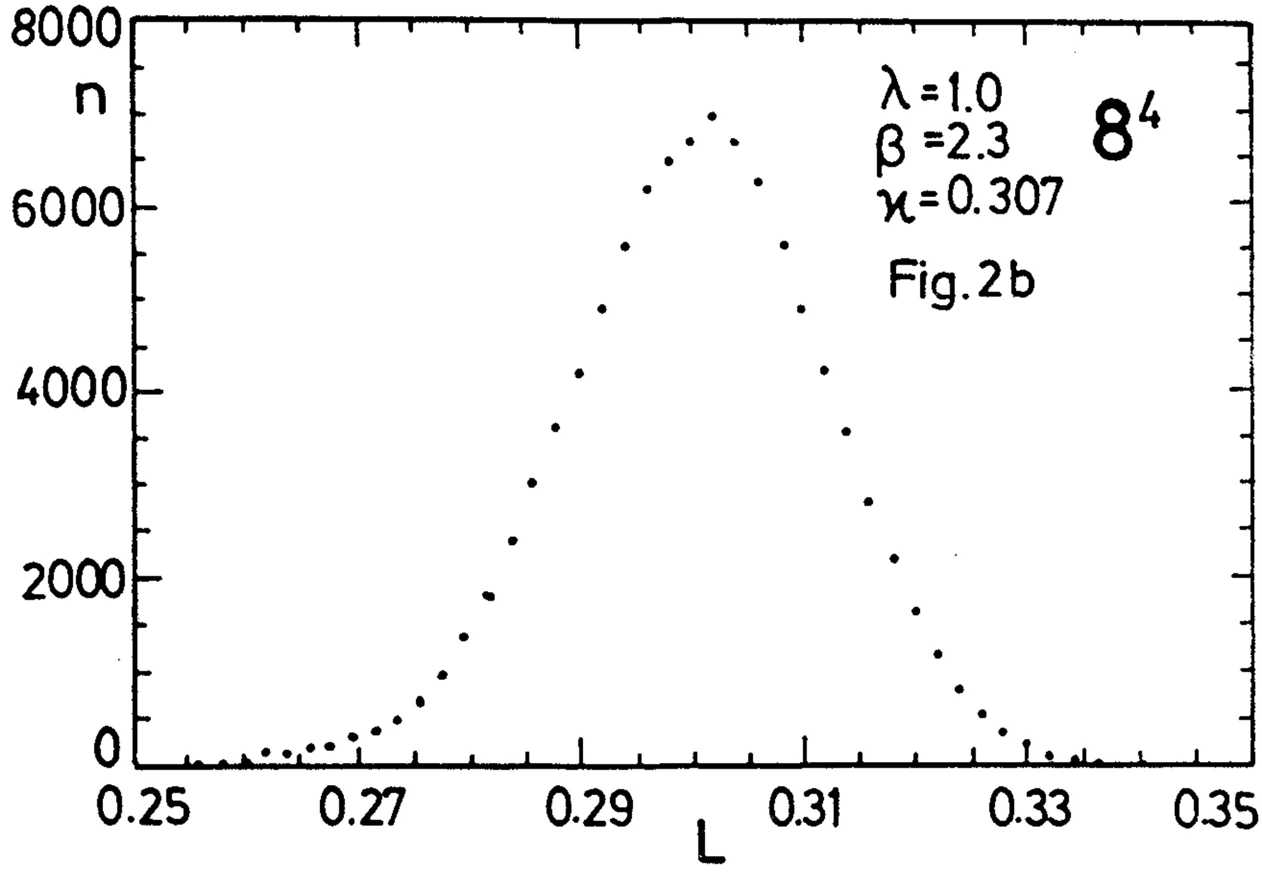
8000
n
6000
4000
2000
0
0.25
0.27
0.29
0.31
0.33
0.35
L
λ =1.0
β =2.3
ϰ =0.307
8⁴
Fig. 2b

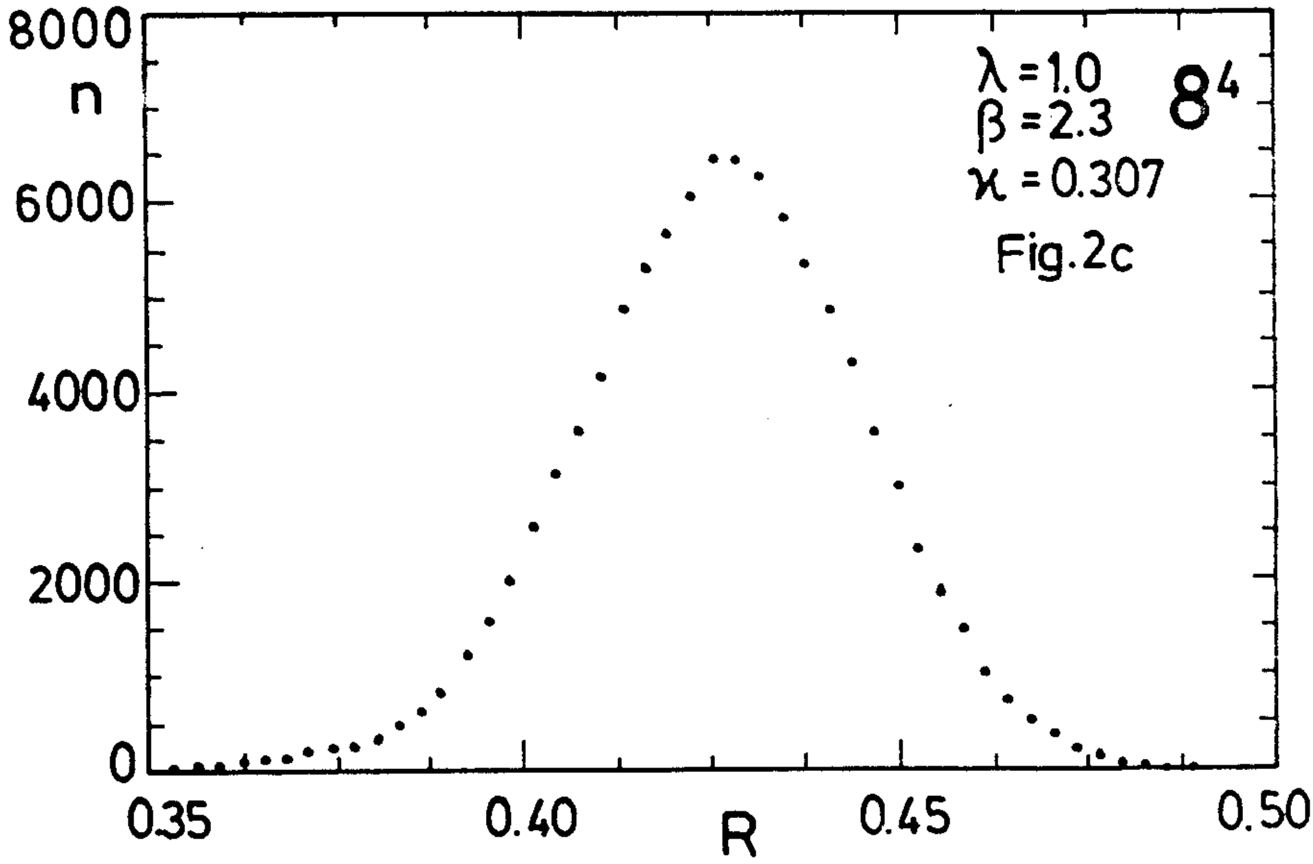

Fig.2c

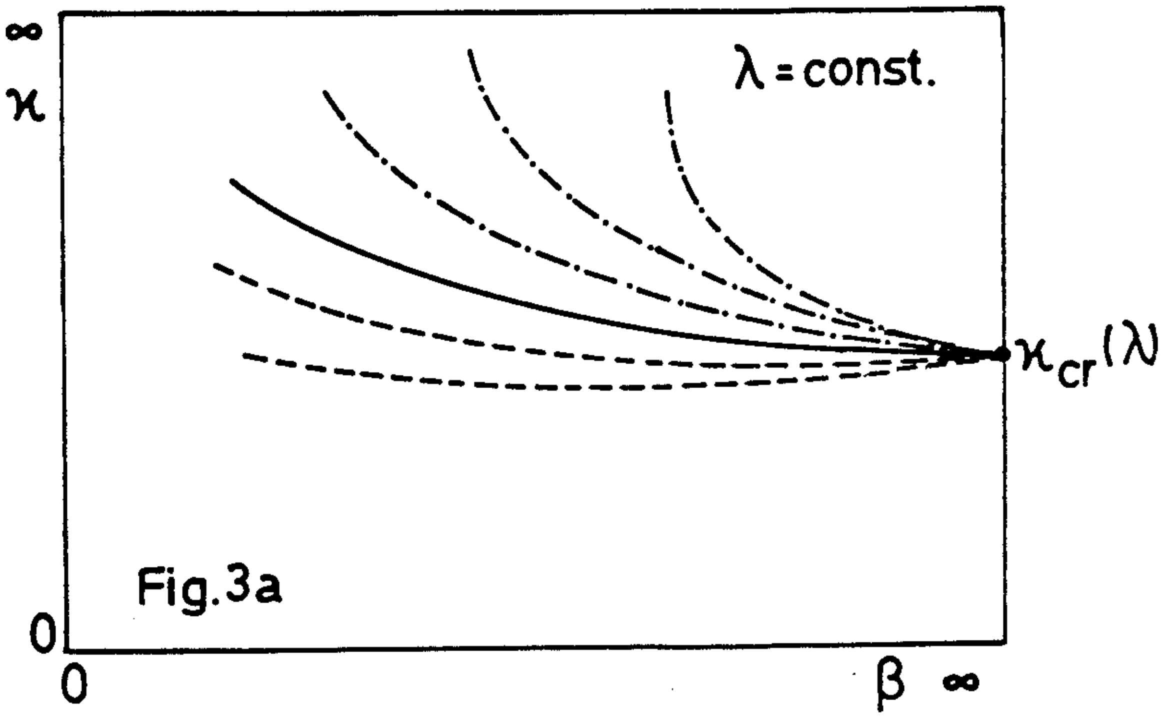

Fig.3a

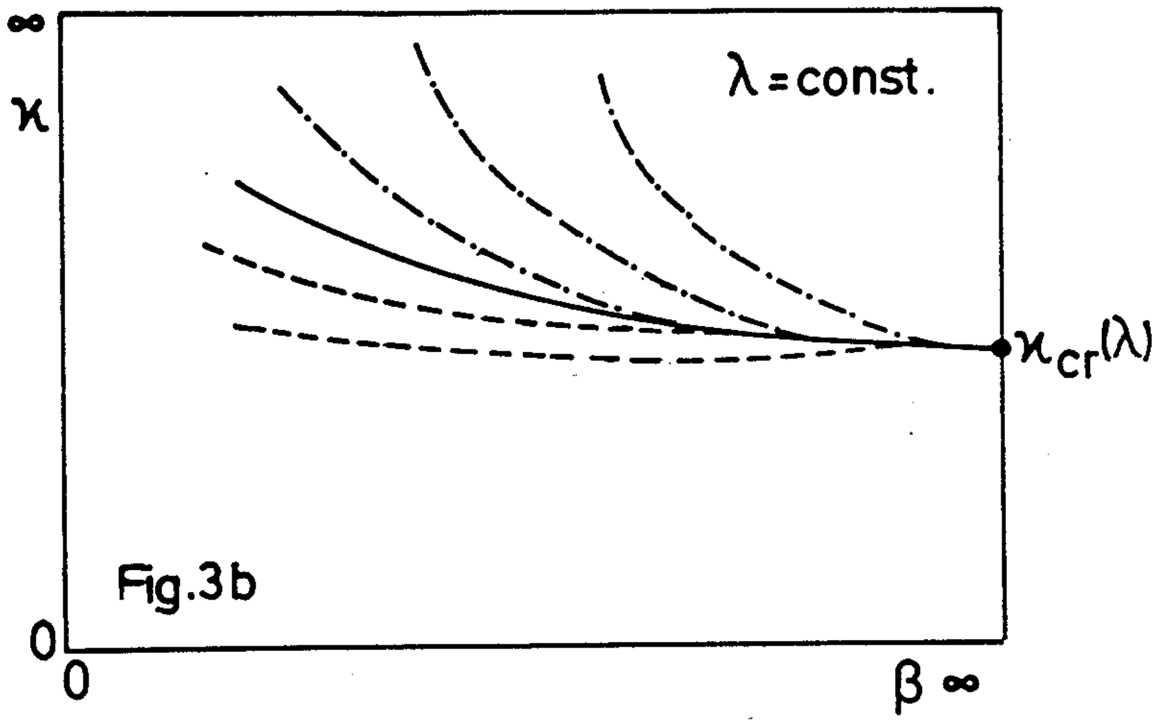

Fig.3b

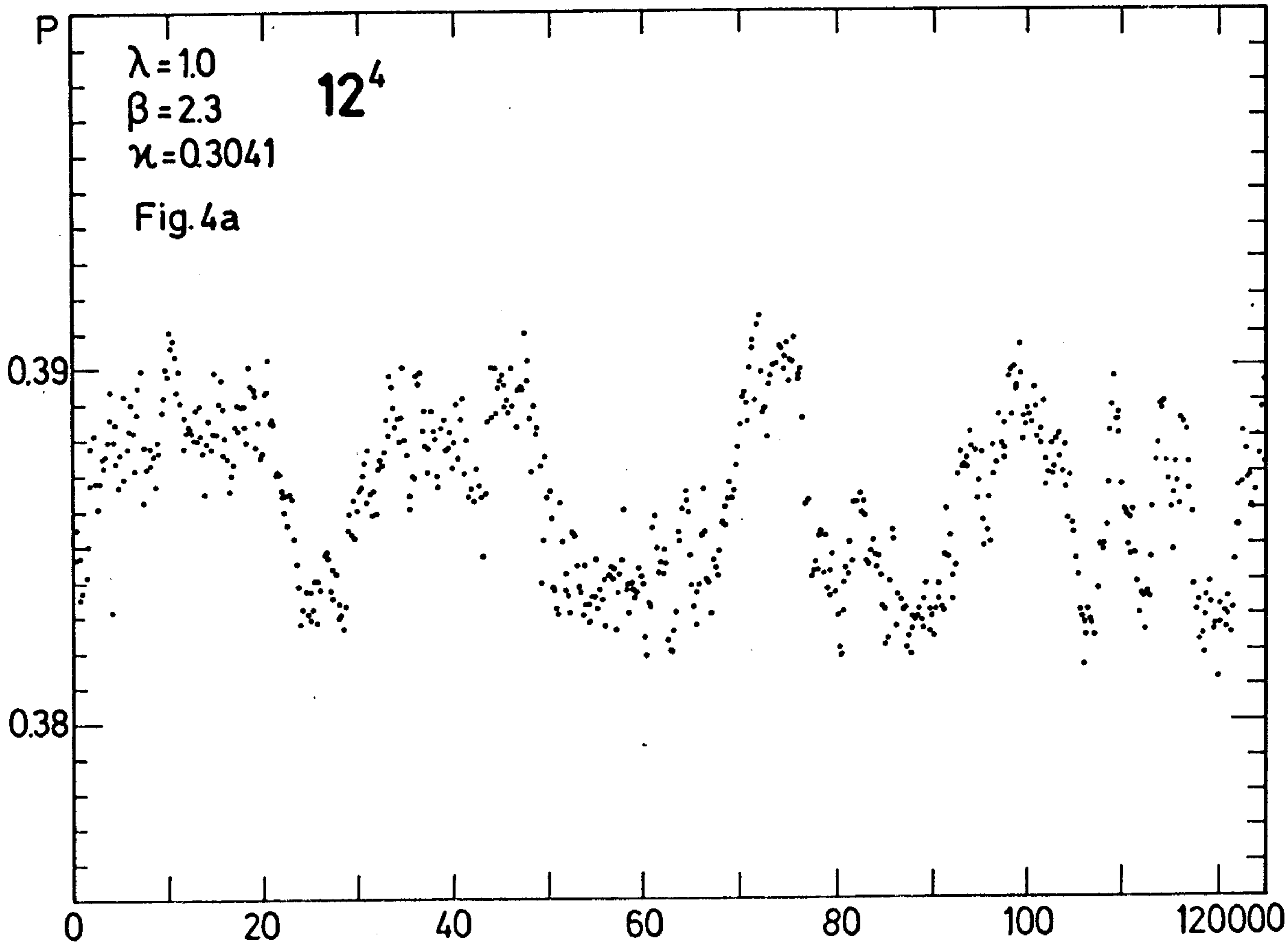
P
λ = 1.0
β = 2.3
κ = 0.3041
Fig. 4a
12^4
0.39
0.38
0
20
40
60
80
100
120000

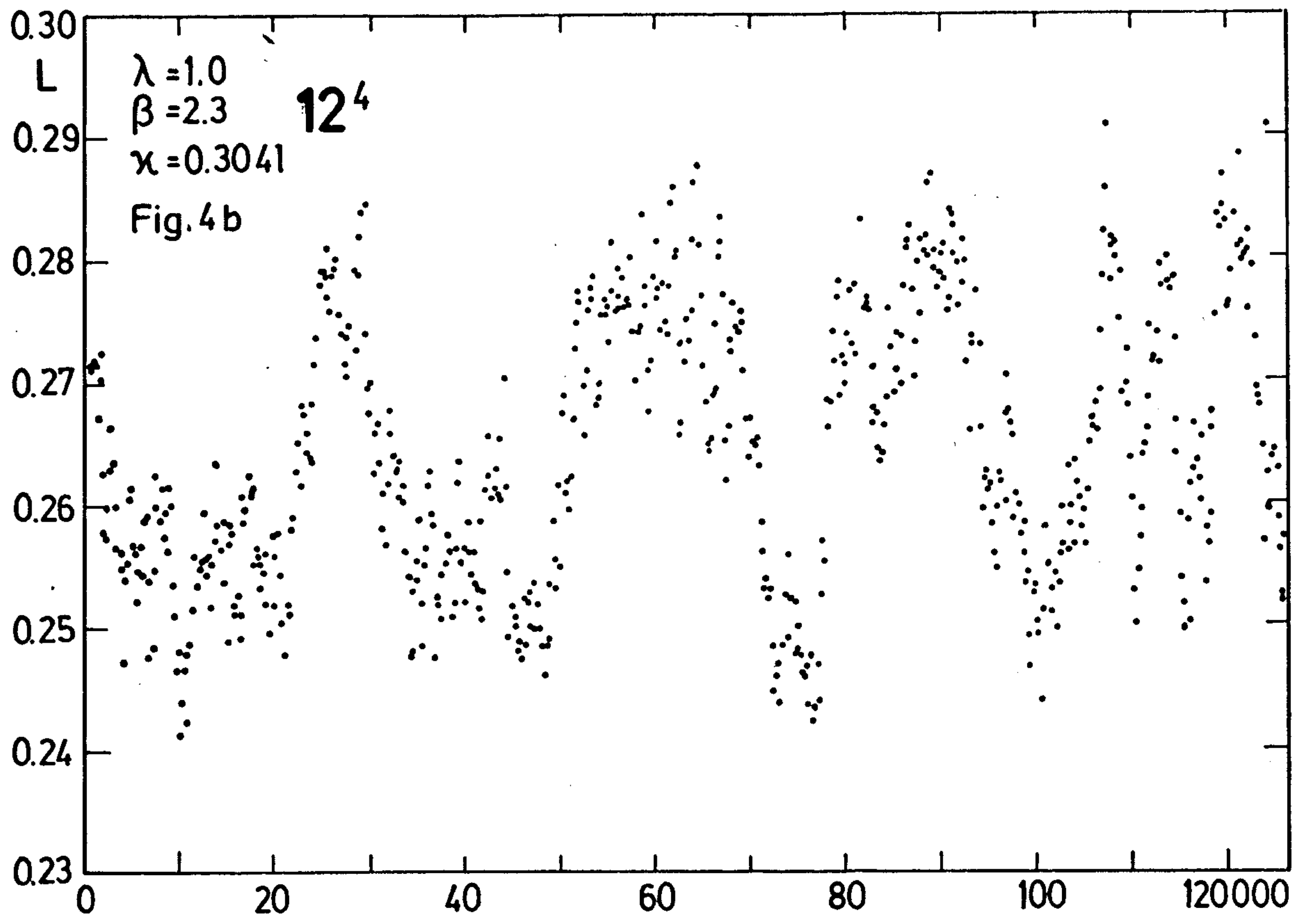
L
λ = 1.0
β = 2.3
χ = 0.3041
12⁴
0.30
0.29
0.28
0.27
0.26
0.25
0.24
0.23
0
20
40
60
80
100
120000

Fig. 4 b

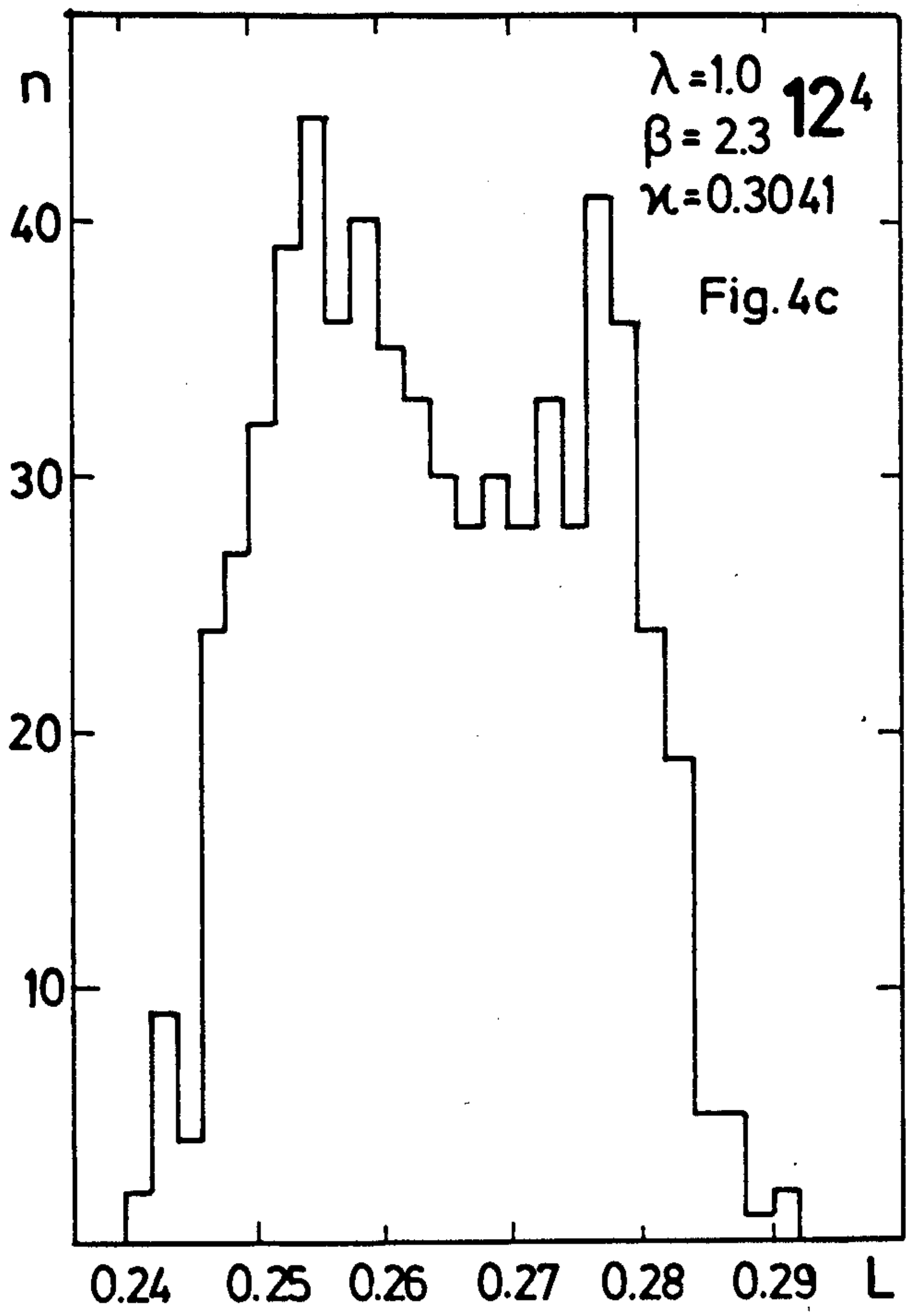

Fig. 4c

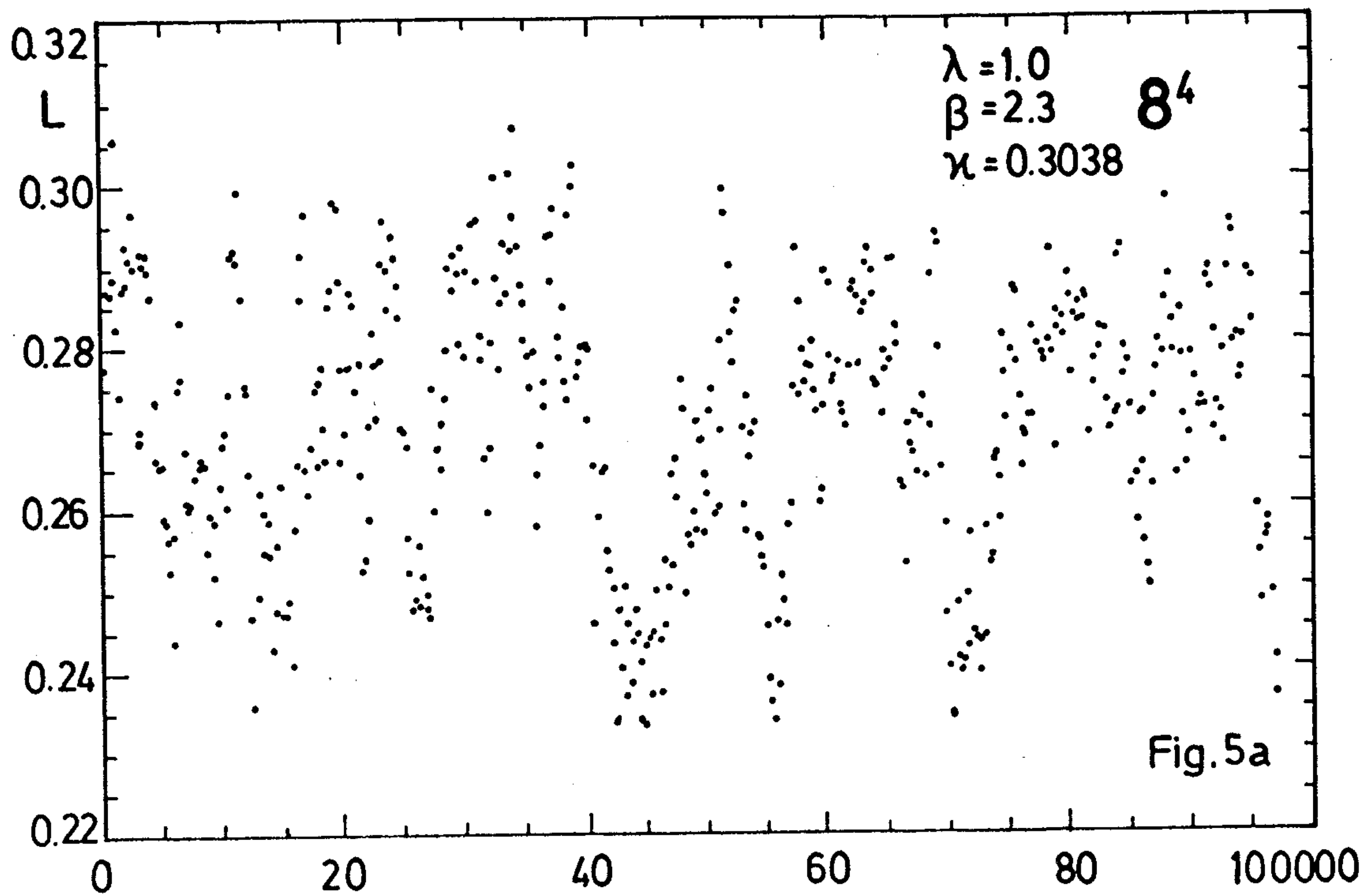
0.32
L
0.30
0.28
0.26
0.24
0.22
0
20
40
60
80
100000
λ = 1.0
β = 2.3
κ = 0.3038
8^4
Fig. 5a

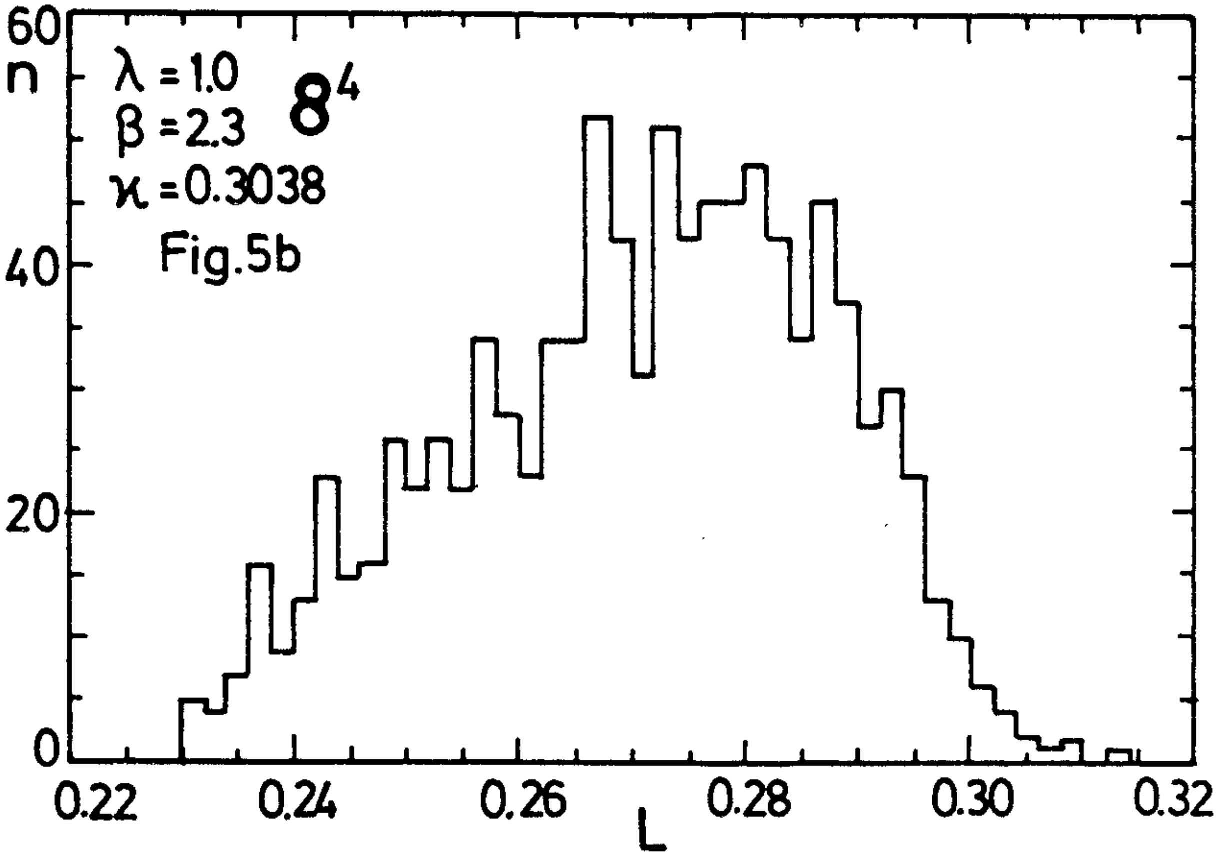

60
n
40
20
0
λ = 1.0
β = 2.3
κ = 0.3038
8⁴
0.22
0.24
0.26
0.28
0.30
0.32
L

Fig.5b

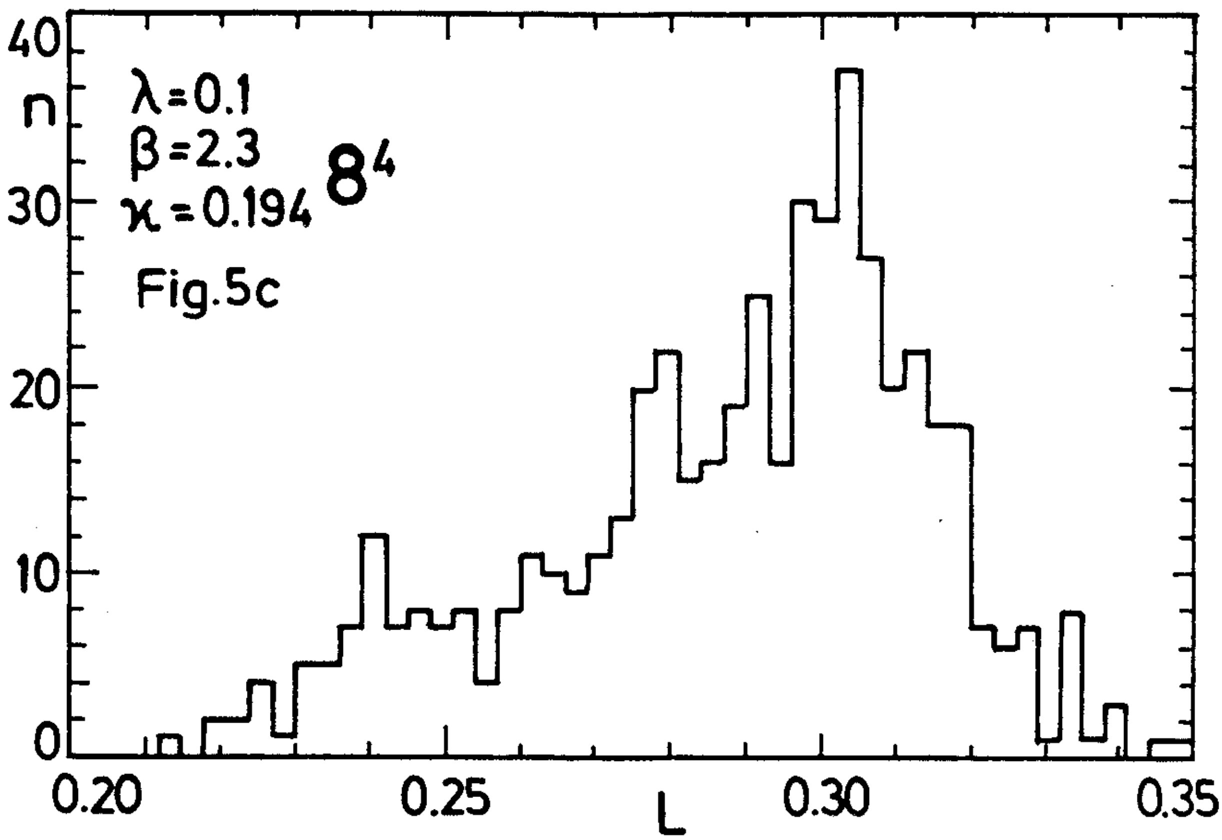

40
n
30
20
10
0
λ = 0.1
β = 2.3
κ = 0.194
8⁴
0.20
0.25
0.30
0.35
L

Fig.5c

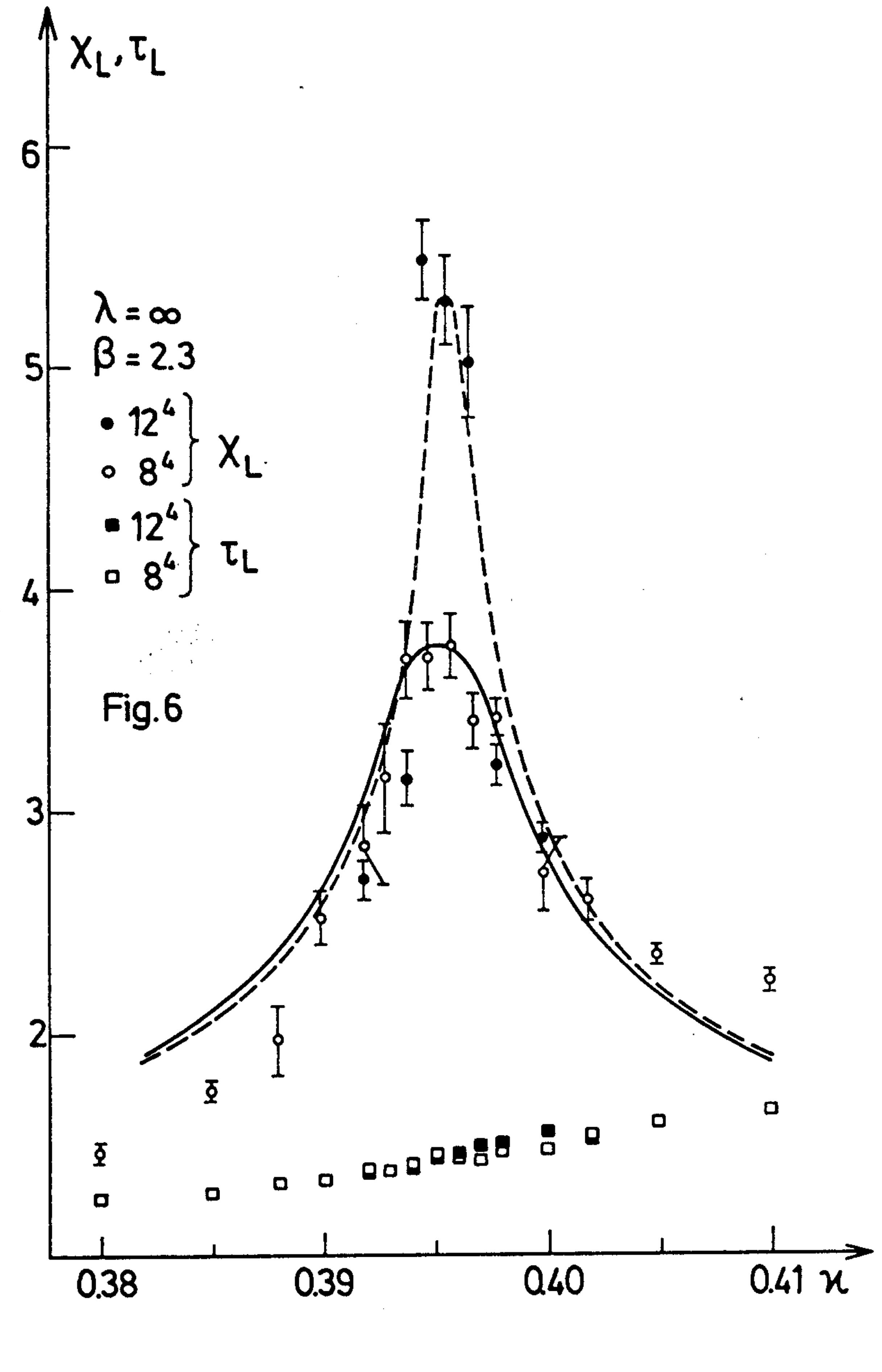

χ_L, τ_L
6
5
4
3
2
$\lambda = \infty$
$\beta = 2.3$
● 12^4
○ 8^4
χ_L
■ 12^4
□ 8^4
τ_L
0.38
0.39
0.40
0.41 κ

Fig. 6